

Joint Recursive Beam and Channel Tracking for 2-dimensional Phased Antenna Arrays

Yu Liu*, Jiahui Li*, Yin Sun[§], Shidong Zhou*

*Dept. of EE, Tsinghua University, Beijing, 100084, China

[§]Dept. of ECE, Auburn University, Auburn AL, 36849, U.S.A

Abstract—Millimeter wave (mmWave) is an attractive candidate for high-speed wireless communication in the future. However, due to the propagation characteristics of mmWave, beam alignment becomes a key challenge in mobile environments. In this paper, we develop a joint 3D recursive beam and channel tracking algorithm that can achieve low tracking error. We discuss the special challenges in optimizing the beamforming matrix of 3D tracking. A general asymptotically optimal beamforming matrix is given to obtain the minimum Cramér-Rao lower bound (CRLB) of beam and channel tracking. The beamforming matrix can be used in different channel environments when antenna number is large enough. In static scenarios, three theorems are developed to prove that the algorithm converges to the minimum CRLB. Simulation results show that our algorithm outperforms several existing algorithms.

I. INTRODUCTION

Due to the broadband character of millimeter-wave, it is promising to support high data rate applications in the future [1]–[3]. In mmWave band, the scattering effect is very weak. Therefore, only one line-of-sight (LOS) path and several reflection paths exist [3] [4]. To compensate for the huge propagation loss, directional beamforming is often used to provide large received signal power.

To reduce the hardware cost of the number of radio frequency (RF) chains and energy consumption, analog beamforming with phased antenna arrays is an attractive opinion [3] [5]–[8]. The narrow beam characteristics of mmWave requires accurate beam direction in beamforming, which can be estimated by large beam training in static scenarios. However, in mobile environments, the beam direction may change fast, making large beam training unacceptable. Therefore, it is a key challenge to track the beam direction with limited pilots in mobile scenarios.

Some algorithms based on compressed sensing have been proposed in [9]–[11], which can reduce the training pilot number. However, these algorithms are designed for static scenarios and the tracking accuracy deteriorates when the beam direction changes fast. Other algorithms [12]–[15] are designed for dynamic environments. However, the beam tracking and the beamforming vector are not optimized in these algorithms, resulting in the poor performance of tracking accuracy.

A recursive beam tracking algorithm is proposed in [16] [17], where one optimal phase shifter is given and proved. However, the assumption that the channel coefficient is known makes it not practical. Thus, another algorithm has been pro-

posed to jointly track channel coefficient and beam direction in [18]. Despite the progress, the algorithm can be only applied into two-dimensional scenarios, where the antenna arrays are placed in a line and the angle-of-arrivals (AoAs) are one-dimensional, leading to the weak practicality. Besides, the optimal beamforming vector obtained by numerical research may not be general for different channel environments.

In this paper, we develop a joint 3D recursive beam and channel tracking algorithm. This algorithm can be applied into 3D scenarios where the two-dimensional phased antenna arrays are placed in a plane and AoAs are two-dimensional. In static scenarios, Cramér-Rao lower bound (CRLB) of beam and channel tracking is obtained, which is a function of beamforming matrix. We discuss the special challenges in optimizing the beamforming matrix of 3D tracking and give a set of general asymptotically optimal beamforming parameters to obtain the minimum CRLB. This beamforming matrix can be used in different channel environments when antenna number is sufficiently large. In addition, three theorems are developed to prove that the algorithm converges to the minimum CRLB with high probability. Simulation results show that our algorithm outperforms several existing algorithms with low tracking error.

II. SYSTEM MODEL

The mmWave channel is sparse with several separated paths. Hence we focus on tracking one of these paths and different paths can be tracked separately by using the same method.

Consider the planar antenna array receiver in Fig. 1, where $M \times N$ antennas are placed in a rectangle, with a distance d_1 between neighboring antennas along x axis and a distance d_2 between neighboring antennas along y axis. Each antenna is connected by a phase shifter. All the phase shifters are connected to the same radio frequency (RF) chain. In time-slot k , N_k pilot symbols arrive at the planar antennas from an angle-of-arrival (AoA) $\theta_k \in [0, \pi/2]$ and $\varphi_k \in [-\pi, \pi]$, where θ_k denotes the elevation angle of arrival and φ_k denotes the azimuth angle of arrival. Hence, the channel vector is given by

$$\mathbf{h}(\beta_k, \mathbf{x}_k) = \beta_k \mathbf{a}(\mathbf{x}_k), \quad (1)$$

where $\beta_k = \beta_k^{\text{re}} + j\beta_k^{\text{im}}$ is the complex channel coefficient, $\mathbf{x}_k = [x_{k,1}, x_{k,2}]^T = \left[\frac{Md_1 \cos(\theta_k) \cos(\varphi_k)}{\lambda}, \frac{Nd_2 \cos(\theta_k) \sin(\varphi_k)}{\lambda} \right]^T$, $\mathbf{a}(\mathbf{x}_k) = [a_{11}(\mathbf{x}_k), a_{12}(\mathbf{x}_k), \dots, a_{mn}(\mathbf{x}_k), \dots, a_{MN}(\mathbf{x}_k)]^T$,

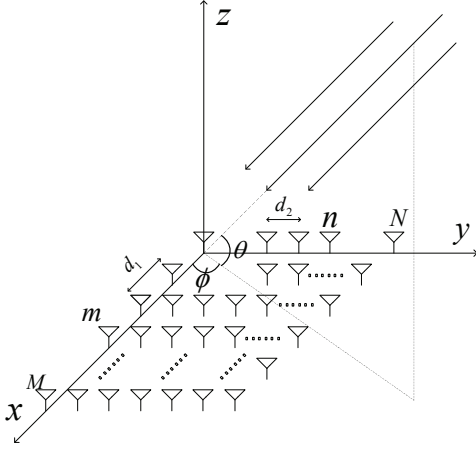


Fig. 1. 2-dimensional phased antenna array.

$a_{mn}(\mathbf{x}_k) = e^{j2\pi(\frac{m-1}{M}x_{k,1} + \frac{n-1}{N}x_{k,2})}$ ($m = 1, 2, \dots, M$, $n = 1, 2, \dots, N$), and λ is the wavelength.

To receive the i -th ($i = 1, 2, \dots, N_k$) pilot symbol in time-slot k , let $\mathbf{w}_{k,i}$ be the beamforming vector provided by the phase shifters:

$$\mathbf{w}_{k,i} = \frac{1}{\sqrt{MN}} \mathbf{a} \left([x_{k,1} + \delta_{k,i1}, x_{k,2} + \delta_{k,i2}]^T \right), \quad (2)$$

where $\mathbf{w}_{k,i}$ is assumed to have the form of steering vector. After phase shifts, the output observation can be given by

$$y_{k,i} = \mathbf{w}_{k,i}^H \mathbf{h}(\mathbf{x}_k) s_p + z_{k,i} = s_p \beta_k \mathbf{w}_{k,i}^H \mathbf{a}(\mathbf{x}_k) + z_{k,i}, \quad (3)$$

where s_p is the pilot symbol, and $z_{k,i} \sim \mathcal{CN}(0, \sigma^2)$ is an *i.i.d.* circularly symmetric complex Gaussian random variable.

We need to track the beam direction \mathbf{x}_k and channel coefficient β_k simultaneously. Given $\Psi_k \triangleq [\beta_k^{\text{re}}, \beta_k^{\text{im}}, x_{k,1}, x_{k,2}]^T$, phase shifts $\mathbf{W}_k \triangleq [\mathbf{w}_{k,1}, \mathbf{w}_{k,2}, \dots, \mathbf{w}_{k,N_k}]$, and the noise $\mathbf{z}_k \triangleq [z_{k,1}, z_{k,2}, \dots, z_{k,N_k}]$, the conditional probability density function of $\mathbf{y}_k \triangleq [y_{k,1}, y_{k,2}, \dots, y_{k,N_k}]^T$ is

$$p(\mathbf{y}_k | \Psi_k, \mathbf{W}_k) = \frac{1}{\pi^{N_k} \sigma^{2N_k}} e^{-\frac{\|\mathbf{y}_k - s_p \beta_k \mathbf{W}_k^H \mathbf{a}(\mathbf{x}_k)\|_2^2}{\sigma^2}}. \quad (4)$$

A beam and channel tracking algorithm provides an analog beamforming matrix \mathbf{W}_k and an estimate $\hat{\Psi}_k \triangleq [\hat{\beta}_k^{\text{re}}, \hat{\beta}_k^{\text{im}}, \hat{x}_{k,1}, \hat{x}_{k,2}]$ of the channel coefficient β_k and beam direction \mathbf{x}_k related to AoA. Let $\zeta = (\mathbf{W}_1, \mathbf{W}_2, \dots, \hat{\Psi}_1, \hat{\Psi}_2, \dots)$ denotes a beam and channel tracking scheme. We consider a particular set Ξ of *causal* beam tracking policies: at the end of time-slot k , the estimate $\hat{\Psi}_k$ of time-slot k and the control action \mathbf{W}_{k+1} of time-slot $k+1$ are determined by the historical control actions $(\mathbf{W}_1, \dots, \mathbf{W}_k)$ and the observations $(\mathbf{y}_1, \dots, \mathbf{y}_k)$ before.

III. PROBLEM FORMULATION AND OPTIMIZATION OF BEAMFORMING MATRIX

In Section III-A, we formulate the problem and give the lower bound of it. Next, the least pilot overhead in each time-slot is discussed. In Section III-C, we explore some features of the optimal beamforming matrix, especially the asymptotically optimal phase shift parameters. Finally, a equilateral triangle

search approach is developed to obtain the minimum CRLB asymptotically in Section III-D.

A. Problem Formulation and Performance Bound

In k -th time-slot, the beam and channel tracking problem is formulated as:

$$\min_{\zeta \in \Xi} \frac{1}{MN} \mathbb{E} \left[\left\| \hat{\beta}_k \mathbf{a}(\hat{\mathbf{x}}_k) - \beta_k \mathbf{a}(\mathbf{x}_k) \right\|_2^2 \right] \quad (5)$$

$$\text{s.t.} \mathbb{E} \left[\hat{\beta}_k \mathbf{a}(\hat{\mathbf{x}}_k) \right] = \beta_k \mathbf{a}(\mathbf{x}_k), \quad (6)$$

where the constraint (6) makes sure that $\mathbf{h}(\hat{\beta}_k, \hat{\mathbf{x}}_k) = \hat{\beta}_k \mathbf{a}(\hat{\mathbf{x}}_k)$ is an unbiased estimation of the channel vector $\mathbf{h}(\beta_k, \mathbf{x}_k) = \beta_k \mathbf{a}(\mathbf{x}_k)$. Problem (5) is hard to solve optimally as a result of the characteristics itself. First of all, we can only obtain part of the system information through observation \mathbf{y}_k , the signal after weighting summation by phase shifts. Second, the beamforming matrix \mathbf{W}_k and the estimation $\hat{\Psi}_k$ need to be optimized. However, both the optimization of control action \mathbf{W}_k and the optimization of estimation $\hat{\Psi}_k$ are non-convex problems.

Such a task in (5) is a huge challenge and hard to be completed in just one paper. Therefore, we make some simplifications and try to take the first step. Consider the static beam tracking, where $\Psi_k = \Psi = [\beta^{\text{re}}, \beta^{\text{im}}, x_1, x_2]^T$ for all time-slots. In order to obtain the CRLB of the channel vector mean square error (MSE) in (5), the Fisher matrix by [19] is introduced as (7), where $\mathbf{g}_k = \mathbf{W}_k^H \mathbf{a}(\mathbf{x})$, $\tilde{\mathbf{g}}_{k1} = \beta \mathbf{W}_k^H \frac{\partial \mathbf{a}(\mathbf{x})}{\partial x_1}$, and $\tilde{\mathbf{g}}_{k2} = \beta \mathbf{W}_k^H \frac{\partial \mathbf{a}(\mathbf{x})}{\partial x_2}$.

The covariance matrix of $\hat{\Psi}_k$ is bounded by the inverse of the Fisher matrix under the condition that $\hat{\Psi}_k$ is an unbiased estimation of Ψ [19]. However, the constraint in (5) does not ensure that condition. In addition, the channel vector in (5) is non-linear to Ψ and the CRLB of MSE can not be given directly. To overcome the difficulties, we introduce the following lemma:

Lemma 1. *If the Fisher matrix is given by (7), then MSE of channel vector in (5) is bounded by CRLB as follows:*

$$\begin{aligned} & \frac{1}{MN} \mathbb{E} \left[\left\| \hat{\beta}_k \mathbf{a}(\hat{\mathbf{x}}_k) - \beta \mathbf{a}(\mathbf{x}) \right\|_2^2 \right] \quad (8) \\ & \geq \frac{1}{MN} \text{Tr} \left\{ \left(\sum_{l=1}^k \mathbf{I}(\Psi, \mathbf{W}_l) \right)^{-1} \sum_{m=1}^M \sum_{n=1}^N \left(\mathbf{v}(m, n, \beta)^H \mathbf{v}(m, n, \beta) \right) \right\}, \end{aligned}$$

$$\text{where } \mathbf{v}(m, n, \beta) \triangleq [1, j, j2\pi \frac{m-1}{M} \beta, j2\pi \frac{n-1}{N} \beta].$$

Proof. see Appendix A.

Lemma 1 tells us the CRLB of the channel vector MSE, which is a function of the beamforming matrices $\mathbf{W}_1, \mathbf{W}_2, \dots, \mathbf{W}_k$. Hence, To obtain the minimum MSE of channel vector, we need to optimize $\mathbf{W}_1, \mathbf{W}_2, \dots, \mathbf{W}_k$ to get the minimum CRLB. Therefore, we can convert problem (5) to (9) in next page, where step (a) is due to the linear additivity of the Fisher matrix [20]. Hence, it is sufficient to optimize just one beamforming matrix \mathbf{W}_k by (9).

$$\begin{aligned} \mathbf{I}(\Psi, \mathbf{W}_k) &\triangleq -\mathbb{E} \left[\frac{\partial \log p(\mathbf{y}_k | \Psi, \mathbf{W}_k)}{\partial \Psi} \cdot \frac{\partial \log p(\mathbf{y}_k | \Psi, \mathbf{W}_k)}{\partial \Psi^T} \right] \\ &= \frac{2|s_p|^2}{\sigma^2} \begin{bmatrix} \|\mathbf{g}_k\|_2^2 & 0 & \text{Re}\{\mathbf{g}_k^H \tilde{\mathbf{g}}_{k1}\} & \text{Re}\{\mathbf{g}_k^H \tilde{\mathbf{g}}_{k2}\} \\ 0 & \|\mathbf{g}_k\|_2^2 & \text{Im}\{\mathbf{g}_k^H \tilde{\mathbf{g}}_{k1}\} & \text{Im}\{\mathbf{g}_k^H \tilde{\mathbf{g}}_{k2}\} \\ \text{Re}\{\mathbf{g}_k^H \tilde{\mathbf{g}}_{k1}\} & \text{Im}\{\mathbf{g}_k^H \tilde{\mathbf{g}}_{k1}\} & \|\tilde{\mathbf{g}}_{k1}\|_2^2 & \text{Re}\{\tilde{\mathbf{g}}_{k1}^H \tilde{\mathbf{g}}_{k2}\} \\ \text{Re}\{\mathbf{g}_k^H \tilde{\mathbf{g}}_{k2}\} & \text{Im}\{\mathbf{g}_k^H \tilde{\mathbf{g}}_{k2}\} & \text{Re}\{\tilde{\mathbf{g}}_{k1}^H \tilde{\mathbf{g}}_{k2}\} & \|\tilde{\mathbf{g}}_{k2}\|_2^2 \end{bmatrix}. \end{aligned} \quad (7)$$

$$\begin{aligned} \text{MSE}_{\text{opt}} &= \min_{\mathbf{w}_1, \mathbf{w}_2, \dots, \mathbf{w}_k} \frac{1}{MN} \text{Tr} \left\{ \left(\sum_{l=1}^k \mathbf{I}(\Psi, \mathbf{W}_l) \right)^{-1} \sum_{m=1}^M \sum_{n=1}^N (\mathbf{v}(m, n, \beta)^H \mathbf{v}(m, n, \beta)) \right\} \\ &\stackrel{(a)}{=} \min_{\mathbf{w}_k} \frac{1}{MN} \text{Tr} \left\{ (k\mathbf{I}(\Psi, \mathbf{W}_k))^{-1} \sum_{m=1}^M \sum_{n=1}^N (\mathbf{v}(m, n, \beta)^H \mathbf{v}(m, n, \beta)) \right\} \\ &= \frac{1}{MN} \text{Tr} \left\{ (k\mathbf{I}(\Psi, \mathbf{W}^*))^{-1} \sum_{m=1}^M \sum_{n=1}^N (\mathbf{v}(m, n, \beta)^H \mathbf{v}(m, n, \beta)) \right\} \\ &\triangleq u(\Psi, \mathbf{W}^*). \end{aligned} \quad (9)$$

B. Least Pilot Overhead

Before optimizing \mathbf{W}_k to get the minimum CRLB in (9), we should determine the size of \mathbf{W}_k . Since $\mathbf{W}_k = [\mathbf{w}_{k,1}, \mathbf{w}_{k,2}, \dots, \mathbf{w}_{k,N_k}]$ is a $MN \times N_k$ matrix, the pilot number N_k should be determined first.

In 2D tracking scenarios where the beam direction is one-dimensional, at least two pilots are required in each time-slot [18]. In 3D scenarios where the beam directional is 2-dimensional, how many pilots are needed to jointly track the beam direction and channel coefficient? It seems that at least 4 pilots are needed in each time-slot since the dimension of beam direction doubles. However, our analysis shows that three pilots are sufficient in each time-slot. To explain that, the following lemma is introduced:

Lemma 2. *If the phase shifts are steering vectors with $\mathbf{w}_{k,i} = \frac{1}{\sqrt{MN}} \mathbf{a}([x_{k,1} + \delta_{k,i1}, x_{k,2} + \delta_{k,i2}]^T)$, then only $N_k + 1$ independent real number equations are obtained by N_k observations neglecting noise at time-slot k .*

Proof. see Appendix B.

Lemma 2 tells us how many independent real observations are obtained after several complex observations. To track the beam direction \mathbf{x}_k and channel coefficient β_k simultaneously (four real variables), we should obtain at least 4 independent real number equations. Therefore, at least three consecutive different observations are required in each time-slot through Lemma 2. Hence, the least pilot overhead in each-time slot is $N_k = 3$. Therefore, we conduct three different observations in each time-slot and $\mathbf{W}_k = [\mathbf{w}_{k,1}, \mathbf{w}_{k,2}, \mathbf{w}_{k,3}]$ is a $MN \times 3$ matrix.

C. Discussion about the Optimal Beamforming Matrix

Consider the optimal beamforming matrix \mathbf{W}^* now. In 2D scenarios, the optimal solution is assumed to be symmetric [18]. Thus there are only one parameter to be optimized and the optimal beamforming matrix is given by numerical

methods. However, the numerical results are not proved to be feasible for other simulation parameters. Extending to 3D scenarios of the beam and channel tracking will bring some new challenges. Due to the steering vector form of $\mathbf{w}_{k,i}$ in Lemma 2 and the pilot number increasing to $N_k = 3$, there are six parameters $\delta_{k,i1}, \delta_{k,i2}$ ($i = 1, 2, 3$) to be determined in 3D scenarios. Therefore, problem (9) is a six-dimensional non-convex problem and it is hard to get analytic results. Even by numerical methods, the optimal parameters obtained may be only suitable for some specific channel coefficients and beam directions, resulting in the poor extensibility. To overcome these difficulties, we introduce the following Lemma:

Lemma 3. *If the phase shifts are steering vectors with $\mathbf{w}_{k,i} = \frac{1}{\sqrt{MN}} \mathbf{a}([x_1 + \delta_{k,i1}, x_2 + \delta_{k,i2}]^T)$, then the optimal parameters $\delta_{k,i1}^*, \delta_{k,i2}^*$ ($i = 1, 2, 3$) of problem (9) are unrelated to channel gain β . Besides, the optimal parameters $\delta_{k,i1}^*, \delta_{k,i2}^*$ ($i = 1, 2, 3$) of problem (9) are irrelevant to the real beam direction $\mathbf{x} \triangleq [x_1, x_2]^T$. Furthermore, the optimal parameters $\delta_{k,i1}^*, \delta_{k,i2}^*$ ($i = 1, 2, 3$) are independent to antenna numbers M, N when M, N tends to infinity.*

Proof. see Appendix C.

Lemma 3 reveals that when antenna number is large, the optimal phase shift parameters $\delta_{k,i1}^*, \delta_{k,i2}^*$ ($i = 1, 2, 3$) converge to determined values for different channel gain β , different beam direction $\mathbf{x} = [x_1, x_2]^T$ and different antenna number $M \times N$. Therefore, the optimal phase shift parameters obtained by numerical results in some particular 3D simulation scenarios (e.g. $M = N = 16, \beta = (1 + j)/\sqrt{2}$ and $\mathbf{x} = [0.1, 0.2]^T$) are feasible to other different channel environments and antenna number. Hence, we can get the general asymptotically optimal phase shift parameters by using numerical research method, which is conducted in the main lobe of the real beam direction:

$$\mathcal{B}(\mathbf{x}) \triangleq (x_1 - 1, x_1 + 1) \times (x_2 - 1, x_2 + 1). \quad (10)$$

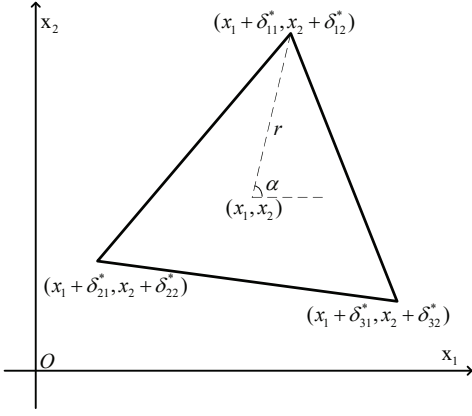


Fig. 2. The equilateral triangle search approach.

D. Equilateral Triangle Search: An Approximate Optimal Approach

To obtain the asymptotically optimal phase shift parameters, coarse search is not enough. However, fine exhaustive search can be unacceptable for a six-dimensional problem in (9) when M and N are large. To reduce the complexity, we need to lower the dimensions. Simulation results show that when M, N are sufficiently large (e.g. $M = N = 16$), the equilateral triangle form in Fig. 2 can approach the optimal phase shifts with the relative error less than 1% between $u(\Psi, \mathbf{W})$ and $u(\Psi, \mathbf{W}^*)$ in (9):

$$\mathbf{w}_{k,i} = \frac{1}{\sqrt{MN}} \mathbf{a} \left(\mathbf{x}_k + r \mathbf{e} \left(\alpha + \frac{2\pi i}{3} - \frac{2\pi}{3} \right) \right), \quad (11)$$

where $\mathbf{e}(s) \triangleq [\cos s, \sin s]^T$, $i = 1, 2, 3$ and $0 < r < 1$.

Therefore, we can use the beamforming vector in (11) to approach the asymptotically optimal phase shift parameters, which leads to the optimization of (9) reducing to a two-dimensional search problem. Then exhaustive search is conducted with the beamforming vector in (11). The CRLB of the channel vector MSE vs r and α is depicted in Fig. 3, where $M = N = 8$, $d_1 = d_2 = \frac{\lambda}{2}$ and the signal-to-noise ratio (SNR) is $\frac{|s_p \beta|^2}{\sigma^2} = 5\text{dB}$. It can be observed that the equilateral triangle form has rotation invariance: the function $u(\Psi, \mathbf{W})$ in (9) doesn't change with angle α in (11). In fact, the rotation invariance keeps when $M > 8$ and $N > 8$. Therefore, set α a constant (e.g. $\alpha = 0$) and the optimization of (9) becomes a one-dimensional search problem to optimize r .

A one-dimension search problem is easier to solve by using numerical methods. Hence, we can obtain the asymptotically optimal r with $\tilde{r}^* = 0.482$ in Fig. 4, where the simulation parameters are set as: antenna number $M = N$, $d_1 = d_2 = \frac{\lambda}{2}$ and the signal-to-noise ratio (SNR) is $\frac{|s_p \beta|^2}{\sigma^2} = 5\text{dB}$. Then the asymptotically optimal beamforming matrix $\tilde{\mathbf{W}}^* \triangleq [\tilde{\mathbf{w}}_{k,1}^*, \tilde{\mathbf{w}}_{k,2}^*, \tilde{\mathbf{w}}_{k,3}^*]$ is given as

$$\tilde{\mathbf{w}}_{k,i}^* = \frac{1}{\sqrt{MN}} \mathbf{a} \left(\mathbf{x}_k + \tilde{r}^* \mathbf{e} \left(\frac{2\pi i}{3} - \frac{2\pi}{3} \right) \right). \quad (12)$$

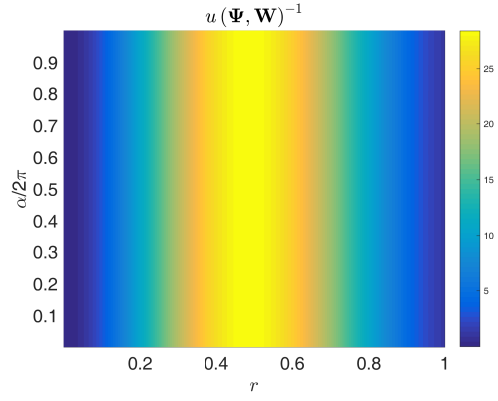


Fig. 3. Rotation invariance of the equilateral triangle form.

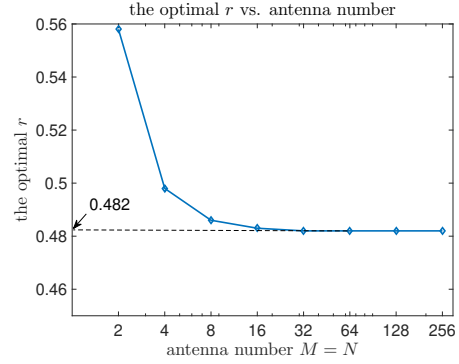


Fig. 4. Asymptotical convergence of the optimal r .

Thus, we obtain the general asymptotically optimal phase shift parameters with $[\tilde{\delta}_{k,i1}^*, \tilde{\delta}_{k,i2}^*]^T = \mathbf{e} \left(\frac{2\pi i}{3} - \frac{2\pi}{3} \right)$ ($i = 1, 2, 3$) to approximate the minimum CRLB in (9).

IV. JOINT 3D RECURSIVE BEAM AND CHANNEL TRACKING

In this section, a joint 3D recursive beam and channel tracking algorithm is developed by using the asymptotically optimal beamforming matrix obtained in (12). Then we show how to obtain the algorithm.

Joint 3D Recursive Beam and Channel Tracking (JRBCCT):

- 1) **Coarse Beam Sweeping:** As shown in Fig. 5, $M \times N$ pilots are received successively. The beamforming vector corresponding to the observation $\tilde{y}_{m,n}$ is $\tilde{\mathbf{w}}_{m,n} = \frac{1}{\sqrt{MN}} \mathbf{a} \left(\left[(2m-1-M) \frac{d_1}{\lambda}, (2n-1-N) \frac{d_2}{\lambda} \right]^T \right)$, $m = 1, 2, \dots, M, n = 1, 2, \dots, N$. Thus, the initial estimate of $\hat{\Psi}_0 = [\hat{\beta}_0^{\text{re}}, \hat{\beta}_0^{\text{im}}, \hat{x}_{0,1}, \hat{x}_{0,2}]^T$ is obtained by:

$$\hat{\mathbf{x}}_0 = \underset{\hat{\mathbf{x}} \in \chi}{\text{argmax}} |\mathbf{a}(\hat{\mathbf{x}})^H \tilde{\mathbf{W}} \tilde{\mathbf{y}}|, \quad \hat{\beta}_0 = \left[\tilde{\mathbf{W}}^H \mathbf{a}(\hat{\mathbf{x}}_0) \right]^+ \tilde{\mathbf{y}}, \quad (13)$$

where $\chi = \left\{ \left[(2m-1-M_0) \frac{M d_1}{\lambda M_0}, (2n-1-N_0) \frac{N d_2}{\lambda N_0} \right]^T \right\}$ ($m = 1, 2, \dots, M_0, n = 1, 2, \dots, N_0$), $M_0 \times N_0$ is the codebook size with $M_0 \geq M$ and $N_0 \geq N$, $\tilde{\mathbf{y}} = [\tilde{y}_{11}, \tilde{y}_{12}, \dots, \tilde{y}_{MN}]^T$, $\tilde{\mathbf{W}} = [\tilde{\mathbf{w}}_{11}, \tilde{\mathbf{w}}_{12}, \dots, \tilde{\mathbf{w}}_{MN}]$, and $\mathbf{X}^+ = (\mathbf{X}^H \mathbf{X})^{-1} \mathbf{X}^H$.

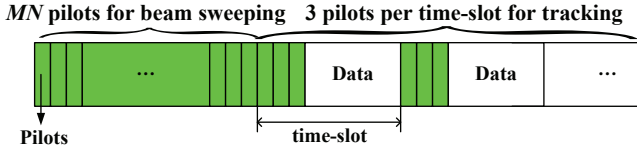


Fig. 5. Frame structure.

2) **Joint 3D Beam and channel tracking:** When beam sweeping is completed, the second stage begins. In time-slot k , three pilots are received using beamforming vector

$$\mathbf{w}_{k,i} = \frac{1}{\sqrt{MN}} \mathbf{a} \left(\hat{\mathbf{x}}_{k-1} + \tilde{r}^* \mathbf{e} \left(\frac{2\pi i}{3} - \frac{2\pi}{3} \right) \right), \quad (14)$$

where $i = 1, 2, 3$ and $\hat{\mathbf{x}}_k \triangleq [\hat{x}_{k,1}, \hat{x}_{k,2}]$. The estimation of the system state $\hat{\Psi}_k = [\hat{\beta}_k^{\text{re}}, \hat{\beta}_k^{\text{im}}, \hat{x}_{k,1}, \hat{x}_{k,2}]$ is updated by (15), where $\mathbf{e}_k = \mathbf{W}_k^H \mathbf{a}(\hat{\mathbf{x}}_{k-1})$, $\tilde{\mathbf{e}}_{k1} = \mathbf{W}_k^H \frac{\partial \mathbf{a}(\hat{\mathbf{x}}_{k-1})}{\partial x_1}$ and $\tilde{\mathbf{e}}_{k2} = \mathbf{W}_k^H \frac{\partial \mathbf{a}(\hat{\mathbf{x}}_{k-1})}{\partial x_2}$. b_k is the step size and will be specified later.

In *Stage 1*, the exhaustive beam sweeping is used and the initial estimation $\hat{\Psi}_0$ is obtained by orthogonal matching pursuits method [11]. The codebook size $M_0 \times N_0$ is adjusted by the accuracy of the initial estimation we need. Simulation result reveals that if $\text{SNR} \geq 0\text{dB}$ and $M_0 = 2M, N_0 = 2N$, the initial estimated beam direction $\hat{\mathbf{x}}_0$ within the main lobe $\mathcal{B}(\mathbf{x})$ can be obtained with high probability.

In *Stage 2*, the joint 3D recursive beam and channel tracking method is inspired by the maximum likelihood (ML) problems:

$$\max_{\hat{\Psi}_k} \left\{ \max_{\mathbf{W}_k} \mathbb{E} \left[\log p(\mathbf{y}_k | \hat{\Psi}_k, \mathbf{W}_k) \right] \middle| \hat{\Psi}_k, \mathbf{W}_1, \dots, \mathbf{W}_k \right\}. \quad (16)$$

A two-layer nested optimization algorithm is proposed to solve (16). In the outer layer, we use the stochastic Newton's method to update $\hat{\Psi}_k$, given by [19],

$$\hat{\Psi}_k = \hat{\Psi}_{k-1} + b_k \mathbf{I} \left(\hat{\Psi}_{k-1}, \mathbf{W}_k \right)^{-1} \frac{\partial \log p(\mathbf{y}_k | \hat{\Psi}_{k-1}, \mathbf{W}_k)}{\partial \hat{\Psi}_{k-1}}. \quad (17)$$

Substituting (4) into (17), we can get

$$\frac{\partial \log p(\mathbf{y}_k | \hat{\Psi}_{k-1}, \mathbf{W}_k)}{\partial \hat{\Psi}_{k-1}} = \frac{2}{\sigma^2} \begin{bmatrix} \text{Re} \left\{ s_p^H \mathbf{e}_k^H (\mathbf{y}_k - s_p \hat{\beta}_{k-1} \mathbf{e}_k) \right\} \\ \text{Im} \left\{ s_p^H \mathbf{e}_k^H (\mathbf{y}_k - s_p \hat{\beta}_{k-1} \mathbf{e}_k) \right\} \\ \text{Re} \left\{ s_p^H \tilde{\mathbf{e}}_{k1}^H (\mathbf{y}_k - s_p \hat{\beta}_{k-1} \mathbf{e}_k) \right\} \\ \text{Re} \left\{ s_p^H \tilde{\mathbf{e}}_{k2}^H (\mathbf{y}_k - s_p \hat{\beta}_{k-1} \mathbf{e}_k) \right\} \end{bmatrix}. \quad (18)$$

In the inner layer, it is equivalent to minimum CRLB to update \mathbf{W}_k , which can be converted to problem (9) and is solved by numerical searching in (12). Substituting (12) and (18) into (17), we get (15) in the end.

V. ASYMPTOTICAL OPTIMALITY ANALYSIS

In this section, we develop three theorems to prove the JRBCT algorithm can converge to the real beam direction with minimum CRLB.

In recursive procedure (15), there exist multiple stable points and these stable points correspond to the local optimal points for our proposed algorithm. We first prove that the real beam direction and channel coefficient. To study these stable points, We rewrite (17) as (19) to study these stable points:

$$\hat{\Psi}_k = \hat{\Psi}_{k-1} + b_k \left(\mathbf{f} \left(\hat{\Psi}_{k-1}, \mathbf{W}_k \right) + \hat{\mathbf{z}}_k \right), \quad (19)$$

where $\mathbf{f} \left(\hat{\Psi}_{k-1}, \mathbf{W}_k \right)$ is defined as follows:

$$\mathbf{f} \left(\hat{\Psi}_{k-1}, \mathbf{W}_k \right) \triangleq \mathbb{E} \left[\mathbf{I} \left(\hat{\Psi}_{k-1}, \mathbf{W}_k \right)^{-1} \frac{\partial \log p(\mathbf{y}_k | \hat{\Psi}_{k-1}, \mathbf{W}_k)}{\partial \hat{\Psi}_{k-1}} \right] \\ = \frac{2|s_p|^2}{\sigma^2} \mathbf{I} \left(\hat{\Psi}_{k-1}, \mathbf{W}_k \right)^{-1} \begin{bmatrix} \text{Re} \left\{ \mathbf{e}_k^H (\beta_k \mathbf{W}_k^H \mathbf{a}(\mathbf{x}_k) - \hat{\beta}_{k-1} \mathbf{e}_k) \right\} \\ \text{Im} \left\{ \mathbf{e}_k^H (\beta_k \mathbf{W}_k^H \mathbf{a}(\mathbf{x}_k) - \hat{\beta}_{k-1} \mathbf{e}_k) \right\} \\ \text{Re} \left\{ \tilde{\mathbf{e}}_{k1}^H (\beta_k \mathbf{W}_k^H \mathbf{a}(\mathbf{x}_k) - \hat{\beta}_{k-1} \mathbf{e}_k) \right\} \\ \text{Re} \left\{ \tilde{\mathbf{e}}_{k2}^H (\beta_k \mathbf{W}_k^H \mathbf{a}(\mathbf{x}_k) - \hat{\beta}_{k-1} \mathbf{e}_k) \right\} \end{bmatrix}, \quad (20)$$

with $\mathbf{e}_k = \mathbf{W}_k^H \mathbf{a}(\hat{\mathbf{x}}_{k-1})$, $\tilde{\mathbf{e}}_{k1} = \mathbf{W}_k^H \frac{\partial \mathbf{a}(\hat{\mathbf{x}}_{k-1})}{\partial x_1}$, $\tilde{\mathbf{e}}_{k2} = \mathbf{W}_k^H \frac{\partial \mathbf{a}(\hat{\mathbf{x}}_{k-1})}{\partial x_2}$, and $\hat{\mathbf{z}}_k$ is given by

$$\hat{\mathbf{z}}_k \triangleq \mathbf{I} \left(\hat{\Psi}_{k-1}, \mathbf{W}_k \right)^{-1} \frac{\partial \log p(\mathbf{y}_k | \hat{\Psi}_{k-1}, \mathbf{W}_k)}{\partial \hat{\Psi}_{k-1}} - \mathbf{f} \left(\hat{\Psi}_{k-1}, \mathbf{W}_k \right). \quad (21)$$

A stable point $\hat{\Psi}_{k-1}$ of $\mathbf{f} \left(\hat{\Psi}_{k-1}, \mathbf{W}_k \right)$ satisfies the following two conditions: 1) $\mathbf{f} \left(\hat{\Psi}_{k-1}, \mathbf{W}_k \right) = 0$; 2) $\frac{\partial \mathbf{f}(\hat{\Psi}_{k-1}, \mathbf{W}_k)}{\partial \hat{\Psi}_{k-1}}$ is negative definite.

The real beam direction and channel coefficient Ψ_k is a stable point: when $\hat{\Psi}_{k-1} = \Psi_k$,

1) $\beta_k \mathbf{W}_k^H \mathbf{a}(\mathbf{x}_k) = \hat{\beta}_{k-1} \mathbf{e}_k$ in (20). Hence, $\mathbf{f}(\Psi_k, \Psi_k) = 0$;

2) $\frac{\partial \mathbf{f}(\Psi_k, \Psi_k)}{\partial \hat{\Psi}_{k-1}} = -\mathbf{J}$ by derivation, where \mathbf{J} is a 4×4 identity matrix. Thus, $\frac{\partial \mathbf{f}(\Psi_k, \Psi_k)}{\partial \hat{\Psi}_{k-1}}$ is negative definite.

Therefore, Ψ_k is a stable point.

Even if Ψ is a stable point, how can we ensure that the tracking procedure converges to Ψ rather than other local optimal points? To resolve the challenge, three theorems are developed here to study the convergence of our algorithm. we adopt diminishing step-size in (22), given by [19], [21], [22]

$$b_k = \frac{\epsilon}{k + K_0}, \quad (22)$$

where $K_0 \geq 0$ and $\epsilon > 0$.

Theorem 1 (Convergence to a Unique Stable Point). *If b_k is given by (22) with $\epsilon > 0$ and $K_0 \geq 0$, then $\hat{\Psi}_k$ converges to a unique stable point with probability one.*

Proof. See Appendix D.

Therefore, for the step-size in (22), $\hat{\Psi}_k$ converges to a unique stable point.

Theorem 2 (Convergence to Real Beam Direction \mathbf{x}). *If (i) $\hat{\mathbf{x}}_0 \in \mathcal{B}(\mathbf{x})$ and (ii) b_k is given by (22) with $\epsilon > 0$, then there exist some $K_0 \geq 0$ and $C > 0$ such that*

$$P(\hat{\mathbf{x}}_k \rightarrow \mathbf{x} | \hat{\mathbf{x}}_0 \in \mathcal{B}(\mathbf{x})) = 1 - 8e^{-\frac{C|s_p|^2}{\epsilon^2 \sigma^2}}. \quad (23)$$

$$\hat{\Psi}_k = \hat{\Psi}_{k-1} + \frac{2}{\sigma^2} b_k \mathbf{I} \left(\hat{\Psi}_{k-1}, \mathbf{W}_k \right)^{-1} \begin{bmatrix} \text{Re} \left\{ s_p^H \mathbf{e}_k^H \left(\mathbf{y}_k - s_p \hat{\beta}_{k-1} \mathbf{e}_k \right) \right\} \\ \text{Im} \left\{ s_p^H \mathbf{e}_k^H \left(\mathbf{y}_k - s_p \hat{\beta}_{k-1} \mathbf{e}_k \right) \right\} \\ \text{Re} \left\{ s_p^H \tilde{\mathbf{e}}_{k1}^H \left(\mathbf{y}_k - s_p \hat{\beta}_{k-1} \mathbf{e}_k \right) \right\} \\ \text{Re} \left\{ s_p^H \tilde{\mathbf{e}}_{k2}^H \left(\mathbf{y}_k - s_p \hat{\beta}_{k-1} \mathbf{e}_k \right) \right\} \end{bmatrix}. \quad (15)$$

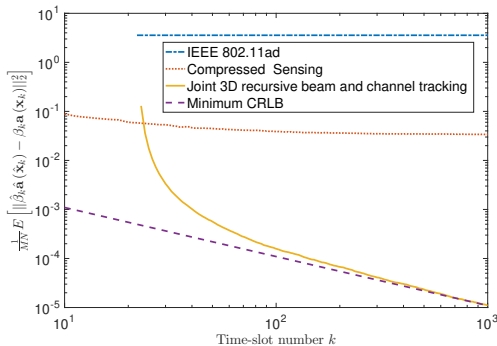


Fig. 6. $\frac{1}{MN} \text{MSE}_{\mathbf{h}(\mathbf{x}_k)}$ vs. time-slot number k in static beam tracking.

Proof. See Appendix E.

At coarse beam sweeping stage of JRBC algorithm, the initial estimation $\hat{\mathbf{x}}_0$ within main lobe $\mathcal{B}(\mathbf{x})$ in (16) can be obtained with high probability. Under the condition $\hat{\mathbf{x}}_0 \in \mathcal{B}(\mathbf{x})$, Theorem 2 tells us the probability of $\hat{\mathbf{x}}_k \rightarrow \mathbf{x}$ is related to $\frac{|s_p|^2}{\epsilon^2 \sigma^2}$. Hence, we can reduce the step-size and increase the transmit SNR $\frac{|s_p|^2}{\sigma^2}$ to make sure that $\hat{\mathbf{x}}_k \rightarrow \mathbf{x}$ with probability one.

Theorem 3 (Convergence to \mathbf{x} with minimum CRLB). *If (i) $\hat{\Psi}_k \rightarrow \Psi_k$ and (ii) b_k is given by (22) with $\epsilon = 1$ and any $K_0 \geq 0$, then*

$$\lim_{k \rightarrow \infty} k \mathbb{E} \left[\left\| \hat{\beta}_k \mathbf{a}(\hat{\mathbf{x}}_k) - \beta_k \mathbf{a}(\mathbf{x}_k) \right\|_2^2 \right] = \text{MSE}_{\text{opt}}. \quad (24)$$

Proof. See Appendix F.

By theorem 3, if $\epsilon = 1$, then we achieve the minimum CRLB asymptotically with high probability.

Proof description for theorem 1-3. Similar to [16]–[18], we use theorem 5.2.1 of [22], chapter 4 of [21], and theorem 6.6.1 of [19] to prove theorem 1-3. Due to space limitation, the detailed proofs are omitted.

VI. NUMERICAL RESULTS

Based on the model in Section II, the parameters are set as: $M = N = 8$, the antenna spacing $d_1 = d_2 = \frac{\lambda}{2}$, the codebook size $M_0 = 2M, N_0 = 2N$, the channel coefficient $\beta_k (\mathbb{E} [|\beta_k|^2] = 1)$, SNR = $\frac{|s_p|^2}{\sigma^2} = 0\text{dB}$. In each time-slot, three pilots are transmitted for all the algorithms to ensure fairness.

In static scenarios, we compare the JRBC algorithm with two other algorithms: the compressed sensing algorithm in [11] and the IEEE 802.11ad algorithm in [12]. The AoA (θ, ϕ) as demonstrated in Section II is chosen evenly and randomly in $\theta \in [0, \frac{\pi}{2}]$, $\phi \in [-\pi, \pi]$. The step-size b_k is set as $b_k = \frac{1}{k}$.

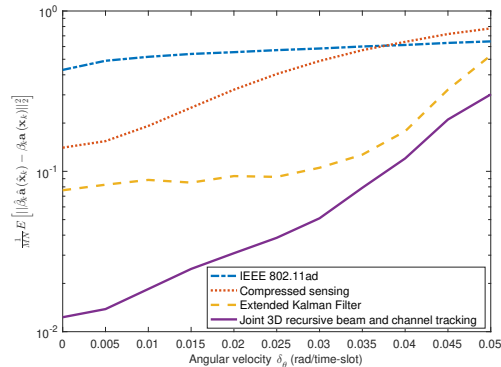


Fig. 7. $\frac{1}{MN} \text{MSE}_{\mathbf{h}(\mathbf{x}_k)}$ vs. angle speed in dynamic beam tracking scenarios.

The channel gain β ($\mathbb{E} [|\beta|^2] = 1$) is modeled as Rician fading with a K-factor $\kappa = 15\text{dB}$ according to the channel model in [23]. Simulation results are averaged over 1000 random system runs. Fig. 6 indicates that the channel vector MSE of JRBC algorithm asymptotically approaches the minimum CRLB and shows much better performance than the two other algorithms.

In dynamic scenarios, we compare the JRBC algorithm with three other algorithms: the compressed sensing algorithm in [11], the IEEE 802.11ad algorithm in [12] and the extended Kalman filter (EKF) method in [15]. The AoA (θ, ϕ) as demonstrated in Section II is modeled in the way of random walk: $\theta(k+1) = \theta(k) + \Delta\theta$, $\phi(k+1) = \phi(k) + \Delta\phi$; $\Delta\theta \sim \mathcal{CN}(0, \delta_\theta^2)$, $\Delta\phi = \Delta\theta$. For each angle speed δ_θ , we can obtain an optimal constant step-size b_k to achieve the least channel vector MSE in JRBC algorithm by using numerical results. Then our step-size is set as the optimal constant step-size for each angle speed. Fig. 6 indicates the JRBC algorithm can achieve lower tracking error than the other three other algorithms.

VII. CONCLUSIONS

We have developed a joint 3D recursive beam and channel tracking algorithm for 2-dimensional phased antenna arrays and give a general optimal beamforming matrix. The theorem of convergence and asymptomatic optimality is established for this algorithm. Simulation results show that our algorithm can achieve lower tracking error than several existing algorithms.

REFERENCES

- [1] Z. Pi and F. Khan, "An introduction to millimeter-wave mobile broadband systems," *IEEE Commun. Mag.*, vol. 49, no. 6, Jun. 2011.
- [2] F. Boccardi, R. W. Heath, A. Lozano, T. L. Marzetta, and P. Popovski, "Five disruptive technology directions for 5G," *IEEE Commun. Mag.*, vol. 52, no. 2, Feb. 2014.
- [3] R. W. Heath, N. González-Prelcic, S. Rangan, W. Roh, and A. M. Sayeed, "An overview of signal processing techniques for millimeter wave MIMO systems," *IEEE J. Sel. Top. Signal Process.*, Apr. 2016.

- [4] T. S. Rappaport, G. R. MacCartney, M. K. Samimi, and S. Sun, "Wide-band millimeter-wave propagation measurements and channel models for future wireless communication system design," *IEEE Trans. Commun.*, vol. 63, no. 9, Sep. 2015.
- [5] S. Sun, T. S. Rappaport, R. W. Heath, A. Nix, and S. Rangan, "MIMO for millimeter-wave wireless communications: Beamforming, spatial multiplexing, or both?" *IEEE Commun. Mag.*, vol. 52, no. 12, Dec. 2014.
- [6] S. Han, C. L. I, Z. Xu, and C. Rowell, "Large-scale antenna systems with hybrid analog and digital beamforming for millimeter wave 5G," *IEEE Commun. Mag.*, vol. 53, no. 1, Jan. 2015.
- [7] A. Puglielli, A. Townley, G. LaCaille, V. Milovanovi, P. Lu, K. Trostkovsky, A. Whitcombe, N. Narevsky, G. Wright, T. Courtade, E. Alon, B. Nikoli, and A. M. Niknejad, "Design of energy- and cost-efficient massive MIMO arrays," *Proc. IEEE*, vol. 104, no. 3, Mar. 2016.
- [8] A. F. Molisch, V. V. Ratnam, S. Han, Z. Li, S. L. H. Nguyen, L. Li, and K. Haneda, "Hybrid beamforming for massive MIMO-a survey," *IEEE Commun. Mag.*, vol. 55, no. 9, Sep. 2017.
- [9] J. Wang, Z. Lan, C.-W. Pyo, T. Baykas, C.-S. Sum, M. A. Rahman, J. Gao, R. Funada, F. Kojima, H. Harada, and S. Kato, "Beam codebook based beamforming protocol for multi-Gbps millimeter-wave WPAN systems," *IEEE J. Sel. Areas Commun.*, vol. 27, no. 8, Oct. 2009.
- [10] A. Alkhateeb, O. E. Ayach, G. Leus, and R. W. Heath, "Channel estimation and hybrid precoding for millimeter wave cellular systems," *IEEE J. Sel. Top. Signal Process.*, vol. 8, no. 5, Oct. 2014.
- [11] A. Alkhateeb, G. Leusz, and R. W. Heath, "Compressed sensing based multi-user millimeter wave systems: How many measurements are needed?" in *IEEE ICASSP*, Apr. 2015.
- [12] IEEE standard, "IEEE 802.11ad WLAN enhancements for very high throughput in the 60 GHz band," Dec. 2012.
- [13] J. Palacios, D. De Donno, and J. Widmer, "Tracking mm-Wave channel dynamics: Fast beam training strategies under mobility," *IEEE INFOCOM*, 2017.
- [14] X. Gao, L. Dai, Y. Zhang, T. Xie, X. Dai, and Z. Wang, "Fast channel tracking for Terahertz beamspace massive MIMO systems," *IEEE Trans. Veh. Technol.*, vol. 66, no. 7, Jul. 2017.
- [15] V. Va, H. Vikalo, and R. W. Heath, "Beam tracking for mobile millimeter wave communication systems," in *IEEE GlobalSIP*, Dec. 2016.
- [16] J. Li, Y. Sun, L. Xiao, S. Zhou, and C. E. Koksall, "Super fast beam tracking in phased antenna arrays," *arXiv preprint arXiv:1710.07873*, 2017.
- [17] —, "Analog beam tracking in linear antenna arrays: Convergence, optimality, and performance," in *51st Asilomar Conference*, 2017.
- [18] J. Li, Y. Sun, L. Xiao, S. Zhou, and A. Sabharwal, "How to mobilize mmWave: A joint beam and channel tracking approach," *arXiv preprint arXiv:1802.02125*, 2018.
- [19] M. B. Nevel'son and R. Z. Has'minskii, *Stochastic approximation and recursive estimation*. American Mathematical Society Providence, 1973.
- [20] H. V. Poor, *An introduction to signal detection and estimation*. New York, NY, USA: Springer-Verlag New York, Inc., 1994.
- [21] V. S. Borkar, *Stochastic approximation: a dynamical systems viewpoint*, 2008.
- [22] H. Kushner and G. G. Yin, *Stochastic approximation and recursive algorithms and applications*. Springer Science & Business Media, 2003, vol. 35.
- [23] S. S. M. K. Samimi, G. R. MacCartney and T. S. Rappaport, "28 GHz millimeter-wave ultrawideband smallscale fading models in wireless channels," in *2016 IEEE VTC Spring*, May. 2016.
- [24] J. M. Holte, "Discrete Gronwall lemma and applications," in *MAA-NCS meeting at the University of North Dakota*, vol. 24, 2009.

APPENDIX A PROOF OF LEMMA 1

If $f(\hat{\mathbf{x}})$ is an unbiased estimation of parameter $f(\mathbf{x})$, then we can obtain

$$\text{Var}[f(\hat{\mathbf{x}})] \geq \frac{\partial f(\mathbf{x})}{\partial \mathbf{x}} \mathbf{I}(\mathbf{x})^{-1} \left(\frac{\partial f(\mathbf{x})}{\partial \mathbf{x}} \right)^H \quad (25)$$

for any first-order continuous derivative function that satisfies $\mathbb{E}[f(\hat{\mathbf{x}})] = f(\mathbf{x})$. Given $f_{mn}(\Psi) = \beta e^{j2\pi(\frac{m-1}{M}x_1 + \frac{n-1}{N}x_2)}$, we can obtain the partial derivative of $f_{mn}(\Psi)$:

$$\left\{ \begin{array}{l} \frac{\partial f_{mn}(\Psi)}{\partial \beta^{re}} = e^{j2\pi(\frac{m-1}{M}x_1 + \frac{n-1}{N}x_2)} \\ \frac{\partial f_{mn}(\Psi)}{\partial \beta^{im}} = j e^{j2\pi(\frac{m-1}{M}x_1 + \frac{n-1}{N}x_2)} \\ \frac{\partial f_{mn}(\Psi)}{\partial x_1} = j2\pi \frac{m-1}{M} \beta e^{j2\pi(\frac{m-1}{M}x_1 + \frac{n-1}{N}x_2)} \\ \frac{\partial f_{mn}(\Psi)}{\partial x_2} = j2\pi \frac{n-1}{N} \beta e^{j2\pi(\frac{m-1}{M}x_1 + \frac{n-1}{N}x_2)} \end{array} \right. \quad (27)$$

Combining (27) (25) and (5), we obtain (26) in next page. Hence, Lemma 1 are proved.

APPENDIX B PROOF OF LEMMA 2

If the phase shifts are steering vectors with $\mathbf{w}_{k,i} = \frac{1}{\sqrt{MN}} \mathbf{a} \left([x_{k,1} + \delta_{k,i1}, x_{k,2} + \delta_{k,i2}]^T \right)$, then we get the two complex equations (28) (29) ignoring noise for the i -th and j -th ($i \neq j$) observations on the top of next page. Separating amplitude and phase angle parts of $y_{k,i}$ and $y_{k,j}$, four real number equations are obtained. The two phase angle equations (30) (31) are given in next page, where $\alpha(y)$ denotes the phase angle of y .

Combining (30) and (31), we can get the following relationship (32) between the phase angle of $y_{k,i}$ and $y_{k,j}$ in next page. The phase angle of $y_{k,i}$ and $y_{k,j}$ are correlated as (32) reveals, for $\delta_{k,i1} - \delta_{k,j1}$ and $\delta_{k,i2} - \delta_{k,j2}$ are already known before tracking. Thus, we can obtain N_k independent amplitude equations and only 1 independent phase angle equation after N_k observations, which are $N_k + 1$ independent real number equations in total.

APPENDIX C PROOF OF LEMMA 3

Due to limit of space, the detailed proofs are not given here. The basic method is block matrix inversion: the Fisher matrix in (7) can be divided into four 2×2 matrices. Then the channel coefficient are canceled in (9) during derivation.

Consider the relationship between the real beam direction \mathbf{x} and the optimal phase shift parameters in problem (9), where only $\mathbf{I}(\Psi, \mathbf{W}_k)$ makes sense. The beamforming matrix $\mathbf{W}_k = [\mathbf{w}_{k,1}, \mathbf{w}_{k,2}, \mathbf{w}_{k,3}, \dots]$ has the steering vector form with $\mathbf{w}_{k,i} = \frac{1}{\sqrt{MN}} \mathbf{a} \left([x_1 + \delta_{k,i1}, x_2 + \delta_{k,i2}]^T \right)$, thus the real beam direction $\mathbf{x} = [x_1, x_2]$ is deduced by derivation in each element of the Fisher matrix. Therefore, the optimal parameters $\delta_{k,i1}^*$, $\delta_{k,i2}^*$ ($i = 1, 2, 3$) of problem (9) are irrelevant to the real beam direction \mathbf{x} .

When antenna number $M \times N$ tends to infinity, the Fisher matrix $\mathbf{I}(\Psi_k, \mathbf{W}_k)$ can be simplified into :

$$\lim_{M, N \rightarrow +\infty} \frac{1}{MN} \mathbf{I}(\Psi, \mathbf{W}_k) = \mathbf{I}_L(\Psi, \mathbf{W}_k), \quad (33)$$

where $\mathbf{I}_L(\Psi, \mathbf{W}_k)$ is a matrix unrelated to M, N . Besides, other items can be simplified into:

$$\lim_{M, N \rightarrow +\infty} \frac{1}{MN} \sum_{m=1}^M \sum_{n=1}^N (\mathbf{v}(m, n, \beta)^H \mathbf{v}(m, n, \beta)) = \mathbf{T}_L(\beta), \quad (34)$$

where $\mathbf{T}_L(\beta)$ is also a matrix unrelated to M, N . Hence, antenna number $M \times N$ only appears in the form of $\frac{1}{MN}$ and does not influence the optimal phase shift parameters.

Therefore, Lemma 3 gets proved.

$$\begin{aligned}
& \frac{1}{MN} \mathbb{E}(\|\hat{\beta}_k \mathbf{a}(\hat{\mathbf{x}}_k) - \beta \mathbf{a}(\mathbf{x})\|_2^2) \\
&= \frac{1}{MN} \sum_{m=1}^M \sum_{n=1}^N \mathbb{E} \left(\left| \hat{\beta}_k e^{j2\pi \left(\frac{m-1}{M} \hat{x}_{k,1} + \frac{n-1}{N} \hat{x}_{k,2} \right)} - \beta e^{j2\pi \left(\frac{m-1}{M} x_1 + \frac{n-1}{N} x_2 \right)} \right|^2 \right) \\
&\geq \frac{1}{MN} \sum_{m=1}^M \sum_{n=1}^N \left(\left[1, j, j2\pi \frac{m-1}{M} \beta, j2\pi \frac{n-1}{N} \beta \right] \left(\sum_{l=1}^k \mathbf{I}(\Psi, \mathbf{W}_l) \right)^{-1} \left[1, j, j2\pi \frac{m-1}{M} \beta, j2\pi \frac{n-1}{N} \beta \right]^H \right) \\
&= \frac{1}{MN} \text{Tr} \left\{ \left(\sum_{l=1}^k \mathbf{I}(\Psi, \mathbf{W}_l) \right)^{-1} \sum_{m=1}^M \sum_{n=1}^N \left(\left[1, j, j2\pi \frac{m-1}{M} \beta, j2\pi \frac{n-1}{N} \beta \right]^H \left[1, j, j2\pi \frac{m-1}{M} \beta, j2\pi \frac{n-1}{N} \beta \right] \right) \right\} \\
&= \frac{1}{MN} \text{Tr} \left\{ \left(\sum_{l=1}^k \mathbf{I}(\Psi, \mathbf{W}_l) \right)^{-1} \sum_{m=1}^M \sum_{n=1}^N \left(\mathbf{v}(m, n, \beta)^H \mathbf{v}(m, n, \beta) \right) \right\}.
\end{aligned} \tag{26}$$

$$y_{k,i}(\beta, x_1, x_2) = \frac{s_p \beta}{\sqrt{MN}} \sum_{m=1}^M \sum_{n=1}^N e^{-j2\pi \left(\frac{(m-1)\delta_{k,i1}}{M} + \frac{(n-1)\delta_{k,i2}}{N} \right)} \tag{28}$$

$$y_{k,j}(\beta, x_1, x_2) = \frac{s_p \beta}{\sqrt{MN}} \sum_{m=1}^M \sum_{n=1}^N e^{-j2\pi \left(\frac{(m-1)\delta_{k,j1}}{M} + \frac{(n-1)\delta_{k,j2}}{N} \right)} \tag{29}$$

$$\alpha(y_{k,i}(\beta, x_1, x_2)) = \alpha(s_p \beta) - \pi \left[\frac{M-1}{M} \delta_{k,i1} + \frac{N-1}{N} \delta_{k,i2} \right]. \tag{30}$$

$$\alpha(y_{k,j}(\beta, x_1, x_2)) = \alpha(s_p \beta) - \pi \left[\frac{M-1}{M} \delta_{k,j1} + \frac{N-1}{N} \delta_{k,j2} \right]. \tag{31}$$

$$\alpha(y_{k,i}(\beta, x_1, x_2)) - \alpha(y_{k,j}(\beta, x_1, x_2)) + \pi \left(\frac{M-1}{M} (\delta_{k,i1} - \delta_{k,j1}) + \frac{N-1}{N} (\delta_{k,i2} - \delta_{k,j2}) \right) = 0. \tag{32}$$

APPENDIX D
PROOF OF THEOREM 1

Recall the beam and channel tracking procedure in (19), where $\mathbf{f}(\hat{\Psi}_{k-1}, \Psi_k)$ are defined in (20) and $\hat{\mathbf{z}}_k$ is defined in (21). We extend $\hat{\mathbf{z}}_k$ to (35)

$$\begin{aligned}
\hat{\mathbf{z}}_k &\triangleq \mathbf{I}(\hat{\Psi}_{k-1}, \mathbf{W}_k)^{-1} \frac{\partial \log p(\mathbf{y}_k | \hat{\Psi}_{k-1}, \mathbf{W}_k)}{\partial \hat{\Psi}_{k-1}} - \mathbf{f}(\hat{\Psi}_{k-1}, \Psi_k) \\
&= \frac{2}{\sigma^2} \mathbf{I}(\hat{\Psi}_{k-1}, \mathbf{W}_k)^{-1} \begin{bmatrix} \text{Re} \{ s_p^H \mathbf{e}_k^H \mathbf{z}_k \} \\ \text{Im} \{ s_p^H \mathbf{e}_k^H \mathbf{z}_k \} \\ \text{Re} \{ s_p^H \tilde{\mathbf{e}}_{k1}^H \mathbf{z}_k \} \\ \text{Re} \{ s_p^H \tilde{\mathbf{e}}_{k2}^H \mathbf{z}_k \} \end{bmatrix}
\end{aligned} \tag{35}$$

Since $\mathbf{z}_k \triangleq [z_{k,1}, z_{k,2}, z_{k,3}]$ is composed of three *i.i.d.* circularly symmetric complex Gaussian random variables, the expectation of $\hat{\mathbf{z}}_k$ is $\mathbb{E}[\hat{\mathbf{z}}_k] = \mathbf{0}$ and the covariance matrix is given by (36), where the step (a) are obtained as follows:

- Since $\mathbf{z}_k = [z_{k,1}, z_{k,2}, z_{k,3}]^T$ consists of three *i.i.d.* circularly symmetric complex Gaussian random variables, we get

$$s_p^H \mathbf{e}_k^H \mathbf{z}_k \sim \mathcal{CN} \left(0, \|s_p \mathbf{e}_k\|_2^2 \sigma^2 \right), \tag{37}$$

$$s_p^H \tilde{\mathbf{e}}_{k1}^H \mathbf{z}_k \sim \mathcal{CN} \left(0, \|s_p \tilde{\mathbf{e}}_{k1}\|_2^2 \sigma^2 \right). \tag{38}$$

$$s_p^H \tilde{\mathbf{e}}_{k2}^H \mathbf{z}_k \sim \mathcal{CN} \left(0, \|s_p \tilde{\mathbf{e}}_{k2}\|_2^2 \sigma^2 \right). \tag{39}$$

- splitting the real part and imaginary part, we obtain

$$\left\{ \begin{aligned}
\text{Re} \{ s_p^H \mathbf{e}_k^H \mathbf{z}_k \} &= \text{Re} \{ s_p^H \mathbf{e}_k^H \} \text{Re} \{ \mathbf{z}_k \} - \text{Im} \{ s_p^H \mathbf{e}_k^H \} \text{Im} \{ \mathbf{z}_k \}, \\
\text{Im} \{ s_p^H \mathbf{e}_k^H \mathbf{z}_k \} &= \text{Re} \{ s_p^H \mathbf{e}_k^H \} \text{Im} \{ \mathbf{z}_k \} + \text{Im} \{ s_p^H \mathbf{e}_k^H \} \text{Re} \{ \mathbf{z}_k \}, \\
\text{Re} \{ s_p^H \tilde{\mathbf{e}}_{k1}^H \mathbf{z}_k \} &= \text{Re} \{ s_p^H \tilde{\mathbf{e}}_{k1}^H \} \text{Re} \{ \mathbf{z}_k \} - \text{Im} \{ s_p^H \tilde{\mathbf{e}}_{k1}^H \} \text{Im} \{ \mathbf{z}_k \}, \\
\text{Re} \{ s_p^H \tilde{\mathbf{e}}_{k2}^H \mathbf{z}_k \} &= \text{Re} \{ s_p^H \tilde{\mathbf{e}}_{k2}^H \} \text{Re} \{ \mathbf{z}_k \} - \text{Im} \{ s_p^H \tilde{\mathbf{e}}_{k2}^H \} \text{Im} \{ \mathbf{z}_k \}, \\
\text{Re} \{ s_p^H \mathbf{e}_k^H s_p \tilde{\mathbf{e}}_{k1} \} &= |s_p|^2 \text{Re} \{ \mathbf{e}_k^H \tilde{\mathbf{e}}_{k1} \} \\
&= \text{Re} \{ s_p^H \mathbf{e}_k^H \} \text{Re} \{ s_p \tilde{\mathbf{e}}_{k1} \} + \text{Im} \{ s_p^H \mathbf{e}_k^H \} \text{Im} \{ s_p \tilde{\mathbf{e}}_{k1} \}, \\
\text{Re} \{ s_p^H \mathbf{e}_k^H s_p \tilde{\mathbf{e}}_{k2} \} &= |s_p|^2 \text{Re} \{ \mathbf{e}_k^H \tilde{\mathbf{e}}_{k2} \} \\
&= \text{Re} \{ s_p^H \mathbf{e}_k^H \} \text{Re} \{ s_p \tilde{\mathbf{e}}_{k2} \} + \text{Im} \{ s_p^H \mathbf{e}_k^H \} \text{Im} \{ s_p \tilde{\mathbf{e}}_{k2} \}, \\
\text{Im} \{ s_p^H \mathbf{e}_k^H s_p \tilde{\mathbf{e}}_{k1} \} &= |s_p|^2 \text{Im} \{ \mathbf{e}_k^H \tilde{\mathbf{e}}_{k1} \} \\
&= \text{Re} \{ s_p^H \mathbf{e}_k^H \} \text{Im} \{ s_p \tilde{\mathbf{e}}_{k1} \} + \text{Im} \{ s_p^H \mathbf{e}_k^H \} \text{Re} \{ s_p \tilde{\mathbf{e}}_{k1} \}, \\
\text{Im} \{ s_p^H \mathbf{e}_k^H s_p \tilde{\mathbf{e}}_{k2} \} &= |s_p|^2 \text{Im} \{ \mathbf{e}_k^H \tilde{\mathbf{e}}_{k2} \} \\
&= \text{Re} \{ s_p^H \mathbf{e}_k^H \} \text{Im} \{ s_p \tilde{\mathbf{e}}_{k2} \} + \text{Im} \{ s_p^H \mathbf{e}_k^H \} \text{Re} \{ s_p \tilde{\mathbf{e}}_{k2} \}, \\
\text{Re} \{ s_p^H \tilde{\mathbf{e}}_{k1}^H s_p \tilde{\mathbf{e}}_{k2} \} &= |s_p|^2 \text{Re} \{ \tilde{\mathbf{e}}_{k1}^H \tilde{\mathbf{e}}_{k2} \} \\
&= \text{Re} \{ s_p^H \tilde{\mathbf{e}}_{k1}^H \} \text{Re} \{ s_p \tilde{\mathbf{e}}_{k2} \} + \text{Im} \{ s_p^H \tilde{\mathbf{e}}_{k1}^H \} \text{Im} \{ s_p \tilde{\mathbf{e}}_{k2} \}
\end{aligned} \right. \tag{40}$$

$$\mathbb{E} \left[(\hat{\mathbf{z}}_k - \mathbb{E}[\hat{\mathbf{z}}_k]) (\hat{\mathbf{z}}_k - \mathbb{E}[\hat{\mathbf{z}}_k])^T \right] = \frac{4}{\sigma^4} \mathbf{I} \left(\hat{\Psi}_{k-1}, \mathbf{W}_k \right)^{-1} \mathbb{E} \left\{ \begin{bmatrix} \text{Re}\{s_p^H \mathbf{e}_k^H \mathbf{z}_k\} \\ \text{Im}\{s_p^H \mathbf{e}_k^H \mathbf{z}_k\} \\ \text{Re}\{s_p^H \tilde{\mathbf{e}}_{k1}^H \mathbf{z}_k\} \\ \text{Re}\{s_p^H \tilde{\mathbf{e}}_{k2}^H \mathbf{z}_k\} \end{bmatrix} \cdot \begin{bmatrix} \text{Re}\{s_p^H \mathbf{e}_k^H \mathbf{z}_k\} \\ \text{Im}\{s_p^H \mathbf{e}_k^H \mathbf{z}_k\} \\ \text{Re}\{s_p^H \tilde{\mathbf{e}}_{k1}^H \mathbf{z}_k\} \\ \text{Re}\{s_p^H \tilde{\mathbf{e}}_{k2}^H \mathbf{z}_k\} \end{bmatrix}^T \right\} \mathbf{I} \left(\hat{\Psi}_{k-1}, \mathbf{W}_k \right)^{-1} \quad (36)$$

$$\stackrel{(a)}{=} \mathbf{I} \left(\hat{\Psi}_{k-1}, \mathbf{W}_k \right)^{-1}$$

• Combining (37), (38), (39) and (40), we can obtain

$$\left\{ \begin{array}{l} \mathbb{E} [\text{Re}\{s_p^H \mathbf{e}_k^H \mathbf{z}_k\}^2] = \mathbb{E} [\text{Im}\{s_p^H \mathbf{e}_k^H \mathbf{z}_k\}^2] = \frac{|s_p|^2 \sigma^2}{2} \|\mathbf{e}_k\|_2^2, \\ \mathbb{E} [\text{Re}\{s_p^H \mathbf{e}_k^H \mathbf{z}_k\} \cdot \text{Im}\{s_p^H \mathbf{e}_k^H \mathbf{z}_k\}] = 0, \\ \mathbb{E} [\text{Re}\{s_p^H \mathbf{e}_k^H \mathbf{z}_k\} \cdot \text{Re}\{s_p^H \tilde{\mathbf{e}}_{k1}^H \mathbf{z}_k\}] = \frac{|s_p|^2 \sigma^2}{2} \text{Re}\{\mathbf{e}_k^H \tilde{\mathbf{e}}_{k1}\}, \\ \mathbb{E} [\text{Re}\{s_p^H \mathbf{e}_k^H \mathbf{z}_k\} \cdot \text{Re}\{s_p^H \tilde{\mathbf{e}}_{k2}^H \mathbf{z}_k\}] = \frac{|s_p|^2 \sigma^2}{2} \text{Re}\{\mathbf{e}_k^H \tilde{\mathbf{e}}_{k2}\}, \\ \mathbb{E} [\text{Im}\{s_p^H \mathbf{e}_k^H \mathbf{z}_k\} \cdot \text{Re}\{s_p^H \tilde{\mathbf{e}}_{k1}^H \mathbf{z}_k\}] = \frac{|s_p|^2 \sigma^2}{2} \text{Im}\{\mathbf{e}_k^H \tilde{\mathbf{e}}_{k1}\}, \\ \mathbb{E} [\text{Im}\{s_p^H \mathbf{e}_k^H \mathbf{z}_k\} \cdot \text{Re}\{s_p^H \tilde{\mathbf{e}}_{k2}^H \mathbf{z}_k\}] = \frac{|s_p|^2 \sigma^2}{2} \text{Im}\{\mathbf{e}_k^H \tilde{\mathbf{e}}_{k2}\}, \\ \mathbb{E} [\text{Re}\{s_p^H \tilde{\mathbf{e}}_{k1}^H \mathbf{z}_k\}^2] = \frac{|s_p|^2 \sigma^2}{2} \|\tilde{\mathbf{e}}_{k1}\|_2^2, \\ \mathbb{E} [\text{Re}\{s_p^H \tilde{\mathbf{e}}_{k2}^H \mathbf{z}_k\}^2] = \frac{|s_p|^2 \sigma^2}{2} \|\tilde{\mathbf{e}}_{k2}\|_2^2, \\ \mathbb{E} [\text{Re}\{s_p^H \tilde{\mathbf{e}}_{k1}^H \mathbf{z}_k\} \cdot \text{Re}\{s_p^H \tilde{\mathbf{e}}_{k2}^H \mathbf{z}_k\}] = \frac{|s_p|^2 \sigma^2}{2} \text{Re}\{\tilde{\mathbf{e}}_{k1}^H \tilde{\mathbf{e}}_{k2}\}. \end{array} \right. \quad (41)$$

Hence, we have

$$\mathbb{E} \left\{ \begin{bmatrix} \text{Re}\{s_p^H \mathbf{e}_k^H \mathbf{z}_k\} \\ \text{Im}\{s_p^H \mathbf{e}_k^H \mathbf{z}_k\} \\ \text{Re}\{s_p^H \tilde{\mathbf{e}}_{k1}^H \mathbf{z}_k\} \\ \text{Re}\{s_p^H \tilde{\mathbf{e}}_{k2}^H \mathbf{z}_k\} \end{bmatrix} \cdot \begin{bmatrix} \text{Re}\{s_p^H \mathbf{e}_k^H \mathbf{z}_k\} \\ \text{Im}\{s_p^H \mathbf{e}_k^H \mathbf{z}_k\} \\ \text{Re}\{s_p^H \tilde{\mathbf{e}}_{k1}^H \mathbf{z}_k\} \\ \text{Re}\{s_p^H \tilde{\mathbf{e}}_{k2}^H \mathbf{z}_k\} \end{bmatrix}^T \right\} = \frac{\sigma^4}{4} \mathbf{I}(\hat{\Psi}_{k-1}, \mathbf{W}_k). \quad (42)$$

• Substituting (42) into (36) yields the result of step (a).

Assume $\{\mathcal{G}_k : k \geq 0\}$ is an increasing sequence of σ -fields of $\{\hat{\Psi}_0, \hat{\Psi}_1, \hat{\Psi}_2, \dots\}$, i.e., $\mathcal{G}_{k-1} \subset \mathcal{G}_k$, where $\mathcal{G}_0 \triangleq \sigma(\hat{\Psi}_0)$ and $\mathcal{G}_k \triangleq \sigma(\hat{\Psi}_0, \hat{\mathbf{z}}_1, \dots, \hat{\mathbf{z}}_k)$ for $k \geq 1$. Because the $\hat{\mathbf{z}}_k$'s are composed of *i.i.d.* circularly symmetric complex Gaussian random variables with zero mean, $\hat{\mathbf{z}}_k$ is independent of \mathcal{G}_{k-1} , and $\hat{\Psi}_{k-1} \in \mathcal{G}_{k-1}$. Hence, we have

$$\begin{aligned} & \mathbb{E} \left[\mathbf{f} \left(\hat{\Psi}_{k-1}, \Psi \right) + \hat{\mathbf{z}}_k \mid \mathcal{G}_{k-1} \right] \\ &= \mathbb{E} \left[\mathbf{f} \left(\hat{\Psi}_{k-1}, \Psi \right) \mid \mathcal{G}_{k-1} \right] + \mathbb{E} [\hat{\mathbf{z}}_k \mid \mathcal{G}_{k-1}] = \mathbf{f} \left(\hat{\Psi}_{k-1}, \Psi \right), \end{aligned} \quad (43)$$

for $k \geq 1$.

Theorem 5.2.1 in [22, Section 5.2.1] gives the conditions that ensure $\hat{\mathbf{x}}_k$ converges to a unique point when there are several points with probability one. Next, we will prove that if the step-size a_k is given by (22) with any $\varepsilon > 0$ and $K_0 \geq 0$, the recursive beam and channel tracking algorithm in (15) satisfies the corresponding conditions below:

1) Step-size requirements:

$$\left\{ \begin{array}{l} a_k = \frac{\varepsilon}{k + K_0} \rightarrow 0, \\ \sum_{k=1}^{\infty} a_k = \sum_{k=1}^{\infty} \frac{\varepsilon}{k + K_0} = \infty, \\ \sum_{k=1}^{\infty} a_k^2 = \sum_{k=1}^{\infty} \frac{\varepsilon^2}{(k + K_0)^2} \leq \sum_{l=1}^{\infty} \frac{\varepsilon^2}{l^2} < \infty. \end{array} \right. \quad (44)$$

2) It is necessary to prove that $\sup_k \mathbb{E} \left[\left\| \mathbf{f} \left(\hat{\Psi}_{k-1}, \Psi \right) + \hat{\mathbf{z}}_k \right\|_2^2 \right] < \infty$.

From (19) and (36), we have

$$\begin{aligned} & \mathbb{E} \left[\left\| \mathbf{f} \left(\hat{\Psi}_{k-1}, \Psi \right) + \hat{\mathbf{z}}_k \right\|_2^2 \right] \\ &= \mathbb{E} \left[\left\| \mathbf{f} \left(\hat{\Psi}_{k-1}, \Psi \right) \right\|_2^2 + 2\mathbf{f} \left(\hat{\Psi}_{k-1}, \Psi \right)^T \hat{\mathbf{z}}_k + \|\hat{\mathbf{z}}_k\|_2^2 \right] \\ &\stackrel{(a)}{=} \mathbb{E} \left[\left\| \mathbf{f} \left(\hat{\Psi}_{k-1}, \Psi \right) \right\|_2^2 \right] + \text{tr} \left\{ \mathbf{I}(\hat{\Psi}_{k-1}, \mathbf{W}_k)^{-1} \right\}, \end{aligned} \quad (45)$$

where step (a) is due to (36) and that $\hat{\mathbf{z}}_k$ is independent of $\mathbf{f} \left(\hat{\Psi}_{k-1}, \Psi \right)$.

From (18) and (20), we have

$$\begin{aligned} \left\| \mathbf{f} \left(\hat{\Psi}_{k-1}, \Psi \right) \right\|_2^2 &\leq \left\| \mathbf{I}(\hat{\Psi}_{k-1}, \mathbf{W}_k)^{-1} \right\|_F^2 \\ &\left\| \frac{2|s_p|^2}{\sigma^2} \begin{bmatrix} \text{Re} \left\{ \mathbf{e}_k^H \left(\beta_k \mathbf{W}_k^H \mathbf{a}(\mathbf{x}_k) - \hat{\beta}_{k-1} \mathbf{e}_k \right) \right\} \\ \text{Im} \left\{ \mathbf{e}_k^H \left(\beta_k \mathbf{W}_k^H \mathbf{a}(\mathbf{x}_k) - \hat{\beta}_{k-1} \mathbf{e}_k \right) \right\} \\ \text{Re} \left\{ \tilde{\mathbf{e}}_{k1}^H \left(\beta_k \mathbf{W}_k^H \mathbf{a}(\mathbf{x}_k) - \hat{\beta}_{k-1} \mathbf{e}_k \right) \right\} \\ \text{Re} \left\{ \tilde{\mathbf{e}}_{k2}^H \left(\beta_k \mathbf{W}_k^H \mathbf{a}(\mathbf{x}_k) - \hat{\beta}_{k-1} \mathbf{e}_k \right) \right\} \end{bmatrix} \right\|_2^2. \end{aligned} \quad (46)$$

As the Fisher information matrix is invertible, we get

$$\left\| \mathbf{I}(\hat{\Psi}_{k-1}, \mathbf{W}_k)^{-1} \right\|_F^2 < \infty. \quad (47)$$

Besides, $\mathbf{W}_k = [\mathbf{w}_{k,1}, \mathbf{w}_{k,2}, \mathbf{w}_{k,3}]$, $\mathbf{e}_k = \mathbf{W}_k^H \mathbf{a}(\hat{\mathbf{x}}_{k-1})$, $\tilde{\mathbf{e}}_{k1} = \mathbf{W}_k^H \frac{\partial \mathbf{a}(\hat{\mathbf{x}}_{k-1})}{\partial x_1}$, $\tilde{\mathbf{e}}_{k2} = \mathbf{W}_k^H \frac{\partial \mathbf{a}(\hat{\mathbf{x}}_{k-1})}{\partial x_2}$, hence we have

$$\begin{aligned} & \left| \mathbf{w}_{k,i}^H \mathbf{a}(\mathbf{x}) \right| \\ &= \left| \frac{1}{\sqrt{MN}} \sum_{m=1}^M \sum_{n=1}^N e^{-j2\pi \left(\frac{(m-1)\delta_{k,i1}}{M} + \frac{(n-1)\delta_{k,i2}}{N} \right)} \right| \\ &\leq \frac{1}{\sqrt{MN}} \sum_{m=1}^M \sum_{n=1}^N \left| e^{-j2\pi \left(\frac{(m-1)\delta_{k,i1}}{M} + \frac{(n-1)\delta_{k,i2}}{N} \right)} \right| \\ &= \sqrt{MN} < \infty \end{aligned} \quad (48)$$

$$\begin{aligned}
& \left| \mathbf{w}_{k,i}^H \frac{\partial \mathbf{a}(\mathbf{x})}{\partial x_1} \right| \\
&= \left| \frac{1}{\sqrt{MN}} \sum_{m=1}^M \sum_{n=1}^N j2\pi \frac{m-1}{M} e^{-j2\pi \left(\frac{(m-1)\delta_{k,i1}}{M} + \frac{(n-1)\delta_{k,i2}}{N} \right)} \right| \\
&\leq \frac{2\pi}{M\sqrt{MN}} \sum_{m=1}^M \sum_{n=1}^N (m-1) \left| e^{-j2\pi \left(\frac{(m-1)\delta_{k,i1}}{M} + \frac{(n-1)\delta_{k,i2}}{N} \right)} \right| \\
&= \sqrt{MN} (M-1) < \infty
\end{aligned} \tag{49}$$

and

$$\begin{aligned}
& \left| \mathbf{w}_{k,i}^H \frac{\partial \mathbf{a}(\mathbf{x})}{\partial x_2} \right| \\
&= \left| \frac{1}{\sqrt{MN}} \sum_{m=1}^M \sum_{n=1}^N j2\pi \frac{n-1}{N} e^{-j2\pi \left(\frac{(m-1)\delta_{k,i1}}{M} + \frac{(n-1)\delta_{k,i2}}{N} \right)} \right| \\
&\leq \frac{2\pi}{N\sqrt{MN}} \sum_{m=1}^M \sum_{n=1}^N (n-1) \left| e^{-j2\pi \left(\frac{(m-1)\delta_{k,i1}}{M} + \frac{(n-1)\delta_{k,i2}}{N} \right)} \right| \\
&= \sqrt{MN} (N-1) < \infty
\end{aligned} \tag{50}$$

for $i = 1, 2, 3$ and all possible $\mathbf{w}_{k,i}$ and \mathbf{x} , thus we can get

$$\left\| \frac{2|s_p|^2}{\sigma^2} \begin{bmatrix} \text{Re} \left\{ \mathbf{e}_k^H \left(\beta_k \mathbf{W}_k^H \mathbf{a}(\mathbf{x}_k) - \hat{\beta}_{k-1} \mathbf{e}_k \right) \right\} \\ \text{Im} \left\{ \mathbf{e}_k^H \left(\beta_k \mathbf{W}_k^H \mathbf{a}(\mathbf{x}_k) - \hat{\beta}_{k-1} \mathbf{e}_k \right) \right\} \\ \text{Re} \left\{ \hat{\mathbf{e}}_{k1}^H \left(\beta_k \mathbf{W}_k^H \mathbf{a}(\mathbf{x}_k) - \hat{\beta}_{k-1} \mathbf{e}_k \right) \right\} \\ \text{Re} \left\{ \hat{\mathbf{e}}_{k2}^H \left(\beta_k \mathbf{W}_k^H \mathbf{a}(\mathbf{x}_k) - \hat{\beta}_{k-1} \mathbf{e}_k \right) \right\} \end{bmatrix} \right\|_2 < \infty. \tag{51}$$

Hence, combining (47) and (51), we have

$$\mathbb{E} \left[\left\| \mathbf{f} \left(\hat{\boldsymbol{\psi}}_{n-1}, \boldsymbol{\psi} \right) \right\|_2^2 \right] < \infty. \tag{52}$$

According to (47), it is clear that $\text{tr} \left\{ \mathbf{I} \left(\hat{\boldsymbol{\Psi}}_{k-1}, \mathbf{W}_k \right)^{-1} \right\} < \infty$. Then, we can get that

$$\sup_n \mathbb{E} \left[\left\| \mathbf{f} \left(\hat{\boldsymbol{\Psi}}_{k-1}, \boldsymbol{\Psi} \right) + \hat{\mathbf{z}}_k \right\|_2^2 \right] < \infty. \tag{53}$$

3) The function $\mathbf{f} \left(\hat{\boldsymbol{\Psi}}_{k-1}, \boldsymbol{\Psi} \right)$ should be continuous with respect to $\hat{\boldsymbol{\Psi}}_{k-1}$.

By using (20), we know that each element of $\mathbf{f} \left(\hat{\boldsymbol{\Psi}}_{k-1}, \boldsymbol{\Psi} \right)$ is continuous with respect to $\hat{\boldsymbol{\Psi}}_{k-1} = \left[\hat{\beta}_{re}, \hat{\beta}_{im}, \hat{x}_1, \hat{x}_2 \right]^T$. Therefore, $\mathbf{f} \left(\hat{\boldsymbol{\Psi}}_{k-1}, \boldsymbol{\Psi} \right)$ is continuous with respect to $\hat{\boldsymbol{\Psi}}_{k-1}$.

4) Let $\boldsymbol{\gamma}_k = \mathbb{E} \left[\mathbf{f} \left(\hat{\boldsymbol{\Psi}}_{k-1}, \boldsymbol{\Psi} \right) + \hat{\mathbf{z}}_k \mid \mathcal{G}_{k-1} \right] - \mathbf{f} \left(\hat{\boldsymbol{\Psi}}_{k-1}, \boldsymbol{\Psi} \right)$. We need to prove that $\sum_{k=1}^{\infty} \|a_k \boldsymbol{\gamma}_k\|_2 < \infty$ with probability one.

From (43), we get $\boldsymbol{\gamma}_k = \mathbf{0}$ for all $k \geq 1$. So we have $\sum_{k=1}^{\infty} \|a_k \boldsymbol{\gamma}_k\|_2 = 0 < \infty$ with probability one.

By Theorem 5.2.1 in [22], $\hat{\mathbf{x}}_k$ converges to a unique stable point within the stable points set with probability one.

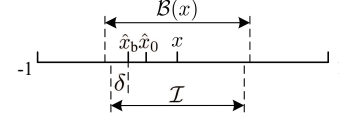


Fig. 8. An illustration of the invariant set \mathcal{I} .

APPENDIX E PROOF OF THEOREM 2

Theorem E is proven in three steps:

Step 1: We will construct two continuous processes based on the discrete process $\hat{\boldsymbol{\psi}}_n = [\hat{\beta}_n^{re}, \hat{\beta}_n^{im}, \hat{x}_n]^T$, i.e., $\bar{\boldsymbol{\psi}}(t) \triangleq [\bar{\beta}^{re}(t), \bar{\beta}^{im}(t), \bar{x}(t)]^T$ and $\tilde{\boldsymbol{\psi}}^n(t) \triangleq [\tilde{\beta}^{re,n}(t), \tilde{\beta}^{im,n}(t), \tilde{x}^n(t)]^T$.

Define the discrete time parameters: $t_0 \triangleq 0$, $t_n \triangleq \sum_{i=1}^n a_i$, $n \geq 1$. The first continuous process $\bar{\boldsymbol{\psi}}(t)$, $t \geq 0$ is the linear interpolation of the sequence $\hat{\boldsymbol{\psi}}_n$, $n \geq 0$, where $\bar{\boldsymbol{\psi}}(t_n) = \hat{\boldsymbol{\psi}}_n$, $n \geq 0$ and $\bar{\boldsymbol{\psi}}(t)$ is given by

$$\bar{\boldsymbol{\psi}}(t) = \bar{\boldsymbol{\psi}}(t_n) + \frac{(t-t_n)}{a_{n+1}} [\bar{\boldsymbol{\psi}}(t_{n+1}) - \bar{\boldsymbol{\psi}}(t_n)], t \in [t_n, t_{n+1}]. \tag{54}$$

The second continuous process $\tilde{\boldsymbol{\psi}}^n(t)$ is a solution of the following ordinary differential equation (ODE):

$$\frac{d\tilde{\boldsymbol{\psi}}^n(t)}{dt} = \mathbf{f} \left(\tilde{\boldsymbol{\psi}}^n(t), \boldsymbol{\psi} \right), \tag{55}$$

for $t \in [t_n, \infty)$, where $\tilde{\boldsymbol{\psi}}^n(t_n) = \bar{\boldsymbol{\psi}}(t_n) = \hat{\boldsymbol{\psi}}_n$, $n \geq 0$. Hence, we have

$$\tilde{\boldsymbol{\psi}}^n(t) = \bar{\boldsymbol{\psi}}(t_n) + \int_{t_n}^t \mathbf{f} \left(\tilde{\boldsymbol{\psi}}^n(v), \boldsymbol{\psi} \right) dv, t \geq t_n. \tag{56}$$

Step 2: By using the continuous processes $\bar{\boldsymbol{\psi}}(t)$ and $\tilde{\boldsymbol{\psi}}^n(t)$, we will form a sufficient condition for the convergence of the discrete process \hat{x}_n .

We first construct a time-invariant set \mathcal{I} that contains the real direction x within the mainlobe, i.e., $x \in \mathcal{I} \subset \mathcal{B}(x)$. Pick δ such that¹

$$\inf_{v \in \partial \mathcal{B}(x), t \geq 0} |v - \tilde{x}^0(t)| = \inf_{v \in \partial \mathcal{B}(x)} |v - \hat{x}_b| > \delta > 0, \tag{57}$$

where $\hat{x}_b = \tilde{x}^0(t_b)$ is the beam direction of the process $\tilde{\boldsymbol{\psi}}^0(t)$ that is closest to the boundary of the mainlobe (see e.g., Fig. 8). Note that when $t \geq t_b$, the solution $\tilde{\boldsymbol{\psi}}^0(t)$ of the ODE (55) will approach the real channel coefficient β and beam direction x monotonically as time t increases. Hence, the invariant set \mathcal{I} can be constructed as follows:

$$\mathcal{I} = \left(x - |x - \hat{x}_b| - \delta, x + |x - \hat{x}_b| + \delta \right) \subset \mathcal{B}(x). \tag{58}$$

An example of the invariant set \mathcal{I} is illustrated in Fig. 8.

Then, we will establish a sufficient condition in Lemma 4 that ensures $\hat{x}_n \in \mathcal{I}$ for $n \geq 0$, and hence from Corollary 2.5 in [21], we can obtain that $\{\hat{x}_n\}$ converges to x . Before giving Lemma 4, let us provide some definitions first:

¹The boundary of the set $\mathcal{B}(x)$ is denoted by $\partial \mathcal{B}(x)$.

- Pick $T > 0$ such that the solution $\tilde{\psi}^0(t), t \geq 0$ of the ODE (55) with $\tilde{\psi}^0(0) = [\hat{\beta}_0^{\text{re}}, \hat{\beta}_0^{\text{im}}, \hat{x}_0]^T$ satisfies $\inf_{v \in \partial \mathcal{B}} |v - \tilde{x}^0(t)| \geq 2\delta$ for $t \geq T$. Since when $t \geq t_b$, $\tilde{x}^0(t)$ will approach the real beam direction x monotonically as time t increases, one possible T is given by

$$T = \arg \min_{t \in [t_b, \infty]} \left| \left[\int_{t_b}^t \mathbf{f}(\tilde{\psi}^0(v), \psi) dv \right]_3 - \delta \right|, \quad (59)$$

where $[\cdot]_i$ obtains the i -th element of the vector.

- Let $T_0 \triangleq 0$ and $T_{m+1} \triangleq \min \{t_i : t_i \geq T_m + T, i \geq 0\}$ for $m \geq 0$. Then $T_{m+1} - T_m \in [T, T + a_1]$ and $T_m = t_{\tilde{n}(m)}$ for some $\tilde{n}(m) \uparrow \infty$, where $\tilde{n}(0) = 0$. Let $\tilde{\psi}^{\tilde{n}(m)}(t)$ denote the solution of ODE (55) for $t \in I_m \triangleq [T_m, T_{m+1}]$ with $\tilde{\psi}^{\tilde{n}(m)}(T_m) = \tilde{\psi}(T_m)$, $m \geq 0$.

Hence, we can obtain the following lemma:

Lemma 4. If $\sup_{t \in I_m} |\tilde{x}(t) - \tilde{x}^{\tilde{n}(m)}(t)| \leq \delta$ for all $m \geq 0$, then $\hat{x}_n \in \mathcal{I}$ for all $n \geq 0$.

Proof. See Appendix G. ■

Step 3: We will derive the probability lower bound for the condition in Lemma 4, which is also a lower bound for $P(\hat{x}_n \rightarrow x | \hat{x}_0 \in \mathcal{B}(x))$.

We will derive the probability lower bound for the condition in Lemma 4, which results in the following lemma:

Lemma 5. If (i) the initial point satisfies $\hat{x}_0 \in \mathcal{B}(x)$, (ii) a_n is given by (22) with any $\alpha > 0$, then there exist $N_0 \geq 0$ and $C > 0$ such that

$$P(\hat{x}_n \in \mathcal{I}, \forall n \geq 0) \geq 1 - 6e^{-\frac{C|s|^2}{\alpha^2 \sigma_0^2}}. \quad (60)$$

Proof. See Appendix H. ■

Finally, by applying Lemma 5 and Corollary 2.5 in [21], we can obtain

$$P(\hat{x}_n \rightarrow x | \hat{x}_0 \in \mathcal{B}) \geq P(\hat{x}_n \in \mathcal{I}, \forall n \geq 0) \geq 1 - 6e^{-\frac{C|s|^2}{\alpha^2 \sigma_0^2}}, \quad (61)$$

which completes the proof of Theorem E.

APPENDIX F PROOF OF THEOREM 3

If the step-size a_k is given by (22) with any $\varepsilon > 0$ and $K_0 \geq 0$, the sufficient conditions are provided by Theorem 6.6.1 [19, Section 6.6] to prove the asymptotic normality of $\sqrt{k}(\hat{\mathbf{x}}_k - \mathbf{x})$, i.e., $\sqrt{k}(\hat{\mathbf{x}}_k - \mathbf{x}) \xrightarrow{d} \mathcal{N}(0, \Sigma_{\mathbf{x}})$. With the condition that $\hat{\Psi}_k \rightarrow \Psi$, we can prove that the recursive beam and channel tracking algorithm satisfies the condition above and obtain the variance Σ as follows:

- 1) Equation (19) is supposed to satisfy: (i) there exists an increasing sequence of σ -fields $\{\mathcal{F}_k : k \geq 0\}$ such that $\mathcal{F}_l \subset \mathcal{F}_k$ for $l < k$, and (ii) the random noise $\hat{\mathbf{z}}_k$ is \mathcal{F}_k -measurable and independent of \mathcal{F}_{k-1} .

As is shown in Appendix D, there exists an increasing

sequence of σ -fields $\{\mathcal{G}_k : k \geq 0\}$, where $\hat{\mathbf{z}}_k$ is measurable with respect to \mathcal{G}_k , i.e., $\mathbb{E}[\hat{\mathbf{z}}_k | \mathcal{G}_k] = \hat{\mathbf{z}}_k$, and is independent of \mathcal{G}_{k-1} , i.e., $\mathbb{E}[\hat{\mathbf{z}}_k | \mathcal{G}_{k-1}] = \mathbb{E}[\hat{\mathbf{z}}_k] = \mathbf{0}$.

- 2) $\hat{\mathbf{x}}_k$ should converge to \mathbf{x} almost surely as $k \rightarrow \infty$.

We assume that $\hat{\Psi}_k \rightarrow \Psi$, hence $\hat{\mathbf{x}}_k$ converges to \mathbf{x} almost surely when $k \rightarrow \infty$.

- 3) The stable condition:

In (20), we rewrite $\mathbf{f}(\hat{\Psi}_{k-1}, \Psi)$ as follows:

$$\mathbf{f}(\hat{\Psi}_{k-1}, \Psi) = \mathbf{C}_1 (\hat{\Psi}_{k-1} - \Psi) + \begin{bmatrix} o(\|\hat{\Psi}_{k-1} - \Psi\|_2) \\ o(\|\hat{\Psi}_{k-1} - \Psi\|_2) \\ o(\|\hat{\Psi}_{k-1} - \Psi\|_2) \end{bmatrix}, \quad (62)$$

, where \mathbf{C}_1 is given by

$$\mathbf{C}_1 = \frac{\partial \mathbf{f}(\hat{\Psi}_{k-1}, \Psi)}{\partial \hat{\Psi}_{k-1}^T} \Big|_{\hat{\Psi}_{k-1} = \Psi} = - \begin{bmatrix} 1 & 0 & 0 \\ 0 & 1 & 0 \\ 0 & 0 & 1 \end{bmatrix}. \quad (63)$$

Then the stable condition is obtained that:

$$\mathbf{E} = \mathbf{C}_1 \cdot \varepsilon + \frac{1}{2} = - \begin{bmatrix} \varepsilon - \frac{1}{2} & 0 & 0 \\ 0 & \varepsilon - \frac{1}{2} & 0 \\ 0 & 0 & \varepsilon - \frac{1}{2} \end{bmatrix} \prec 0, \quad (64)$$

which leads to $\varepsilon > \frac{1}{2}$.

- 4) The noise vector $\hat{\mathbf{z}}_k$ satisfies:

$$\mathbb{E}[\|\hat{\mathbf{z}}_k\|_2^2] = \text{tr}(\mathbf{I}(\hat{\Psi}_{k-1}, \mathbf{W}_k)^{-1}) < \infty, \quad (65)$$

and

$$\lim_{v \rightarrow \infty} \sup_{k \geq 1} \int_{\|\hat{\mathbf{z}}_k\|_2 > v} \|\hat{\mathbf{z}}_k\|_2^2 p(\hat{\mathbf{z}}_k) d\hat{\mathbf{z}}_k = 0. \quad (66)$$

Let

$$\begin{aligned} \mathbf{F} &= \lim_{k \rightarrow \infty} \mathbb{E}[\hat{\mathbf{z}}_k \hat{\mathbf{z}}_k^T] \\ &\quad \hat{\Psi}_k \rightarrow \Psi \\ &\stackrel{(a)}{=} \lim_{k \rightarrow \infty} \mathbf{I}(\hat{\Psi}_k, \mathbf{W}_{k+1})^{-1} = \mathbf{I}(\Psi, \mathbf{W}^*)^{-1}, \\ &\quad \hat{\Psi}_k \rightarrow \Psi \end{aligned} \quad (67)$$

where step (a) is obtained from (36).

By Theorem 6.6.1 [19, Section 6.6], we have

$$\sqrt{k + K_0} (\hat{\Psi}_k - \Psi) \xrightarrow{d} \mathcal{N}(0, \Sigma),$$

where

$$\begin{aligned} \Sigma &= \alpha^2 \cdot \int_0^\infty e^{\mathbf{E}v} \mathbf{F} e^{\mathbf{E}^H v} dv \\ &= \frac{\varepsilon^2}{2\varepsilon - 1} \mathbf{I}(\Psi, \mathbf{W}^*)^{-1}. \end{aligned} \quad (68)$$

Due to that $\lim_{k \rightarrow \infty} \sqrt{(k + K_0)/k} = 1$, we have

$$\sqrt{k} (\hat{\Psi}_k - \Psi) \rightarrow \sqrt{k} \cdot \sqrt{\frac{k + K_0}{k}} (\hat{\Psi}_k - \Psi) \xrightarrow{d} \mathcal{N}(0, \Sigma),$$

if $k \rightarrow \infty$. Thus, we can get

$$\sqrt{k} \left(\hat{\Psi}_k - \Psi \right) \xrightarrow{d} \mathcal{N}(0, \Sigma). \quad (69)$$

By adapting $\alpha = 1$ in (68), we can obtain

$$\sqrt{k} \left(\hat{\Psi}_k - \Psi \right) \xrightarrow{d} \mathcal{N}(0, \mathbf{I}(\psi, \mathbf{W}^*)^{-1}). \quad (70)$$

Combining (25), (70) and (9), we can conclude that

$$\lim_{k \rightarrow \infty} k \mathbb{E} \left[\left\| \hat{\beta}_k \mathbf{a}(\hat{\mathbf{x}}_k) - \beta_k \mathbf{a}(\mathbf{x}_k) \right\|_2^2 \right] = u(\Psi, \mathbf{W}^*) = \text{MSE}_{\text{opt}}. \quad (71)$$

APPENDIX G PROOF OF LEMMA 4

When $m = 0$, $\tilde{x}^{\tilde{n}(0)}(T_0) = \bar{x}(T_0) = \hat{x}_0$. There are two symmetrical cases: (i) $\hat{x}_0 < x$ and (ii) $\hat{x}_0 > x$.

Case 1 ($\hat{x}_0 < x$): We will first prove that $\bar{x}(t) \in \mathcal{I} = (x - |x - \hat{x}_b| - \delta, x + |x - \hat{x}_b| + \delta)$ for all $t \in I_0$.

If $|\bar{x}(t) - \tilde{x}^{\tilde{n}(0)}(t)| \leq \delta$ for all $t \in I_0$, then we have

$$-\delta \leq \bar{x}(t) - \tilde{x}^{\tilde{n}(0)}(t) \leq \delta. \quad (72)$$

What's more, due to the definition of \hat{x}_b in (57), we get

$$\hat{x}_b \leq x, \tilde{x}^{\tilde{n}(0)}(t) - \hat{x}_b \geq 0, x - \tilde{x}^{\tilde{n}(0)}(t) \geq 0, \quad (73)$$

for all $t \in I_0$. By using (72) and (73), we can obtain

$$\begin{aligned} & \bar{x}(t) - (x - |x - \hat{x}_b| - \delta) \\ &= \bar{x}(t) - (\hat{x}_b - \delta) \\ &= \left[\bar{x}(t) - \tilde{x}^{\tilde{n}(0)}(t) \right] + \left[\tilde{x}^{\tilde{n}(0)}(t) - \hat{x}_b \right] + \delta \geq 0, \end{aligned} \quad (74)$$

and

$$\begin{aligned} & (x + |x - \hat{x}_b| + \delta) - \bar{x}(t) \\ &= (2x - \hat{x}_b + \delta) - \bar{x}(t) \\ &= (x - \hat{x}_b) + [x - \bar{x}(t)] + \delta \\ &= (x - \hat{x}_b) + \left[x - \tilde{x}^{\tilde{n}(0)}(t) \right] + \left[\tilde{x}^{\tilde{n}(0)}(t) - \bar{x}(t) \right] + \delta \\ &\geq 0, \end{aligned} \quad (75)$$

which result in $\bar{x}(t) \in \mathcal{I}$ for all $t \in I_0$.

Then, we consider the initial value $\bar{x}(T_1)$ for the next time interval I_1 . With the T given by (59), we have

$$x - \hat{x}_b \geq \tilde{x}^{\tilde{n}(0)}(T_1) - \hat{x}_b \geq \tilde{x}^{\tilde{n}(0)}(T) - \hat{x}_b \geq \delta. \quad (76)$$

By using (72), (73) and (76), we get

$$\begin{aligned} & \bar{x}(T_1) - (x - |x - \hat{x}_b|) \\ &= \bar{x}(T_1) - \hat{x}_b \\ &= \left[\bar{x}(T_1) - \tilde{x}^{\tilde{n}(0)}(T_1) \right] + \left[\tilde{x}^{\tilde{n}(0)}(T_1) - \hat{x}_b \right] \geq 0, \end{aligned} \quad (77)$$

and

$$\begin{aligned} & (x + |x - \hat{x}_b|) - \bar{x}(T_1) \\ &= (2x - \hat{x}_b) - \bar{x}(T_1) \\ &= (x - \hat{x}_b) + [x - \bar{x}(T_1)] \\ &= (x - \hat{x}_b) + \left[x - \tilde{x}^{\tilde{n}(0)}(T_1) \right] + \left[\tilde{x}^{\tilde{n}(0)}(T_1) - \bar{x}(T_1) \right] \\ &\geq 0, \end{aligned} \quad (78)$$

which result in $\bar{x}(T_1) \in [x - |x - \hat{x}_b|, x + |x - \hat{x}_b|]$.

Case 2 ($\hat{x}_0 > x$): Owing to symmetric property, we can use the same method as (74), (75), (77) and (78) to obtain that $\bar{x}(t) \in \mathcal{I}$ for all $t \in I_0$ and $\bar{x}(T_1) \in [x - |x - \hat{x}_b|, x + |x - \hat{x}_b|]$.

When $m = 1$, $\tilde{x}^{\tilde{n}(1)}(T_1) = \bar{x}(T_1) \in [x - |x - \hat{x}_b|, x + |x - \hat{x}_b|]$. If $\bar{x}(T_1) < x$ and $|\bar{x}(t) - \tilde{x}^{\tilde{n}(1)}(t)| \leq \delta$, then for all $t \in I_1$, we have $\bar{x}(T_1) \geq \hat{x}_b$, $\tilde{x}^{\tilde{n}(1)}(t) - \hat{x}_b \geq 0$, $x - \tilde{x}^{\tilde{n}(1)}(t) \geq 0$, and

$$x - \hat{x}_b \geq \tilde{x}^{\tilde{n}(1)}(T_2) - \hat{x}_b \geq \tilde{x}^{\tilde{n}(1)}(T_1 + T) - \hat{x}_b \geq \delta.$$

Similar to (74), (75), (77) and (78), we can get $\bar{x}(t) \in \mathcal{I}$ for all $t \in I_1$ and $\bar{x}(T_2) \in [x - |x - \hat{x}_b|, x + |x - \hat{x}_b|]$, which are also true for the case that $\bar{x}(T_1) > x$.

Hence, we can use the same method to prove the cases of $m \geq 2$, which finally yields $\bar{x}(t) \in \mathcal{I}$ for all $t \in I_m$ and $m \geq 0$. Since $\bar{x}(t_n) = \hat{x}_n$ for all $n \geq 0$, we can obtain that $\hat{x}_n \in \mathcal{I}$ for all $n \geq 0$, which completes the proof.

APPENDIX H PROOF OF LEMMA 5

The following lemmas are needed to prove Lemma 5:

Lemma 6. Given T by (59) and

$$n_T \triangleq \inf \{i \in \mathbb{Z} : t_{n+i} \geq t_n + T\}. \quad (79)$$

If there exists a constant $C > 0$, which satisfies

$$\begin{aligned} & \left\| \bar{\psi}(t_{n+m}) - \tilde{\psi}^n(t_{n+m}) \right\|_2 \\ &\leq L \sum_{i=1}^m a_{n+i} \left\| \bar{\psi}(t_{n+i-1}) - \tilde{\psi}^n(t_{n+i-1}) \right\|_2 + C, \end{aligned} \quad (80)$$

for all $n \geq 0$ and $1 \leq m \leq n_T$, then

$$\sup_{t \in [t_n, t_{n+n_T}]} \left\| \bar{\psi}(t) - \tilde{\psi}^n(t) \right\|_2 \leq \frac{C_{\mathbf{f}} a_{n+1}}{2} + C e^{L(T+a_1)}, \quad (81)$$

where L and $C_{\mathbf{f}}$ are defined in (86) and (87) separately.

Proof. See Appendix I. ■

Lemma 7 (Lemma 4 [16]). If $\{M_i : i = 1, 2, \dots\}$ satisfies that: (i) M_i is Gaussian distributed with zero mean, and (ii) M_i is a martingale in i , then

$$P \left(\sup_{0 \leq i \leq k} |M_i| > \eta \right) \leq 2 \exp \left\{ -\frac{\eta^2}{2 \text{Var}[M_k]} \right\}, \quad (82)$$

for any $\eta > 0$.

Lemma 8 (Lemma 5 [16]). If given a constant $C > 0$, then

$$G(v) = \frac{1}{v} \exp \left[-\frac{C}{v} \right], \quad (83)$$

is increasing for all $0 < v < C$.

Let $\xi_0 \triangleq \mathbf{0}$ and $\xi_n \triangleq \sum_{m=1}^n a_m \hat{\mathbf{z}}_m$, $n \geq 1$, where $\hat{\mathbf{z}}_m$ is given in (35). With (54) and (56), we have for t_{n+m} , $1 \leq m \leq n_T$,

$$\begin{aligned} \bar{\psi}(t_{n+m}) &= \bar{\psi}(t_n) + \sum_{i=1}^m a_{n+i} \mathbf{f}(\bar{\psi}(t_{n+i-1}), \psi) \\ &\quad + (\xi_{n+m} - \xi_n), \end{aligned} \quad (84)$$

and

$$\begin{aligned} \tilde{\psi}^n(t_{n+m}) &= \tilde{\psi}^n(t_n) + \int_{t_n}^{t_{n+m}} \mathbf{f}(\tilde{\psi}^n(v), \psi) dv \\ &= \tilde{\psi}^n(t_n) + \sum_{i=1}^m a_{n+i} \mathbf{f}(\tilde{\psi}^n(t_{n+i-1}), \psi) \\ &\quad + \int_{t_n}^{t_{n+m}} [\mathbf{f}(\tilde{\psi}^n(v), \psi) - \mathbf{f}(\tilde{\psi}^n(\underline{v}), \psi)] dv, \end{aligned} \quad (85)$$

where $\underline{v} \triangleq \max\{t_n : t_n \leq v, n \geq 0\}$ for $v \geq 0$.

To bound $\int_{t_n}^{t_{n+m}} [\mathbf{f}(\tilde{\psi}^n(v), \psi) - \mathbf{f}(\tilde{\psi}^n(\underline{v}), \psi)] dv$ on the RHS of (85), we obtain the Lipschitz constant of function $\mathbf{f}(\mathbf{v}, \psi)$ considering the first variable \mathbf{v} , given by

$$L \triangleq \sup_{\mathbf{v}_1 \neq \mathbf{v}_2} \frac{\|\mathbf{f}(\mathbf{v}_1, \psi) - \mathbf{f}(\mathbf{v}_2, \psi)\|_2}{\|\mathbf{v}_1 - \mathbf{v}_2\|_2}. \quad (86)$$

Similar to (46), for any $t \geq t_n$, we can obtain that there exists a constant $0 < C_f < \infty$ such that

$$\|\mathbf{f}(\tilde{\psi}^n(t), \psi)\|_2 \leq C_f. \quad (87)$$

Hence, we have

$$\begin{aligned} &\left\| \int_{t_n}^{t_{n+m}} [\mathbf{f}(\tilde{\psi}^n(v), \psi) - \mathbf{f}(\tilde{\psi}^n(\underline{v}), \psi)] dv \right\|_2 \\ &\leq \int_{t_n}^{t_{n+m}} \left\| \mathbf{f}(\tilde{\psi}^n(v), \psi) - \mathbf{f}(\tilde{\psi}^n(\underline{v}), \psi) \right\|_2 dv \\ &\stackrel{(a)}{\leq} \int_{t_n}^{t_{n+m}} L \left\| \tilde{\psi}^n(v) - \tilde{\psi}^n(\underline{v}) \right\|_2 dv \\ &\stackrel{(b)}{\leq} \int_{t_n}^{t_{n+m}} L \left\| \int_{\underline{v}}^v \mathbf{f}(\tilde{\psi}^n(s), \psi) ds \right\|_2 dv \\ &\leq \int_{t_n}^{t_{n+m}} \int_{\underline{v}}^v L \left\| \mathbf{f}(\tilde{\psi}^n(s), \psi) \right\|_2 ds dv \\ &\stackrel{(c)}{\leq} \int_{t_n}^{t_{n+m}} \int_{\underline{v}}^v C_f L ds dv = \int_{t_n}^{t_{n+m}} C_f L (v - \underline{v}) dv \\ &= \sum_{i=1}^m \int_{t_{n+i-1}}^{t_{n+i}} C_f L (v - t_{n+i-1}) dv \\ &= \sum_{i=1}^m \frac{C_f L (t_{n+i} - t_{n+i-1})^2}{2} = \frac{C_f L}{2} \sum_{i=1}^m a_{n+i}^2, \end{aligned} \quad (88)$$

where step (a) is due to (86), step (b) is due to the definition in (56), and step (c) is due to (87). Then, by subtracting $\tilde{\psi}^n(t_{n+m})$ in (85) from $\bar{\psi}(t_{n+m})$ in (84) and taking norms, the following inequality can be obtained from (86) and (88) for $n \geq 0, 1 \leq m \leq n_T$:

$$\begin{aligned} &\left\| \bar{\psi}(t_{n+m}) - \tilde{\psi}^n(t_{n+m}) \right\|_2 \\ &\leq L \sum_{i=1}^m a_{n+i} \left\| \bar{\psi}(t_{n+i-1}) - \tilde{\psi}^n(t_{n+i-1}) \right\|_2 \\ &\quad + \frac{C_f L}{2} \sum_{i=1}^m a_{n+i}^2 + \|\xi_{n+m} - \xi_n\|_2 \\ &\leq L \sum_{i=1}^m a_{n+i} \left\| \bar{\psi}(t_{n+i-1}) - \tilde{\psi}^n(t_{n+i-1}) \right\|_2 \\ &\quad + \frac{C_f L}{2} \sum_{i=1}^{n_T} a_{n+i}^2 + \sup_{1 \leq m \leq n_T} \|\xi_{n+m} - \xi_n\|_2. \end{aligned} \quad (89)$$

Applying Lemma 6 to (89) and letting

$$C = \frac{C_f L}{2} \sum_{i=1}^{n_T} a_{n+i}^2 + \sup_{1 \leq m \leq n_T} \|\xi_{n+m} - \xi_n\|_2,$$

yields

$$\begin{aligned} &\sup_{t \in [t_n, t_{n+n_T}]} \left\| \bar{\psi}(t) - \tilde{\psi}^n(t) \right\|_2 \\ &\leq C_e \left\{ \frac{C_f L}{2} [b(n) - b(n + n_T)] \right. \\ &\quad \left. + \sup_{1 \leq m \leq n_T} \|\xi_{n+m} - \xi_n\|_2 \right\} + \frac{C_f a_{n+1}}{2}, \end{aligned} \quad (90)$$

where $C_e \triangleq e^{L(T+a_1)}$, and $b(n) \triangleq \sum_{i>n} a_i^2$. Letting $n = \tilde{n}(m)$ in (90), we have $n+n_T = \tilde{n}(m+1)$ due to the definition of $T_{m+1} = t_{\tilde{n}(m+1)}$ in Step 2 of Appendix E and

$$\begin{aligned} &\sup_{t \in I_m} \left\| \bar{\psi}(t) - \tilde{\psi}^{\tilde{n}(m)}(t) \right\|_2 \\ &\leq C_e \left\{ \frac{C_f L}{2} [b(\tilde{n}(m)) - b(\tilde{n}(m+1))] \right. \\ &\quad \left. + \sup_{\tilde{n}(m) \leq k \leq \tilde{n}(m+1)} \|\xi_k - \xi_{\tilde{n}(m)}\|_2 \right\} + \frac{C_f a_{\tilde{n}(m)+1}}{2}. \end{aligned} \quad (91)$$

Suppose that the step size $\{a_n : n > 0\}$ satisfies

$$C_e \frac{C_f L}{2} [b(\tilde{n}(m)) - b(\tilde{n}(m+1))] + \frac{C_f a_{\tilde{n}(m)+1}}{2} < \frac{\delta}{2}, \quad (92)$$

for $m \geq 0$.

Given $\sup_{t \in I_m} |\bar{x}(t) - \tilde{x}^{\tilde{n}(m)}(t)| > \delta$, we can obtain from (91) and (92) that

$$\begin{aligned} & \sup_{\tilde{n}(m) \leq k \leq \tilde{n}(m+1)} \|\xi_k - \xi_{\tilde{n}(m)}\|_2 \\ & \geq \frac{1}{C_e} \left(\sup_{t \in I_m} \|\tilde{\psi}(t) - \tilde{\psi}^{\tilde{n}(m)}(t)\|_2 - \frac{C_f L}{2} [b(\tilde{n}(m)) \right. \\ & \quad \left. - b(\tilde{n}(m+1))] - \frac{C_f a_{\tilde{n}(m+1)}}{2} \right) \\ & > \frac{1}{C_e} \left(\sup_{t \in I_m} |\bar{x}(t) - \tilde{x}^{\tilde{n}(m)}(t)| - \frac{\delta}{2} \right) \\ & > \frac{\delta}{2C_e}. \end{aligned}$$

Then, we get

$$\begin{aligned} & P \left(\sup_{t \in I_m} |\bar{x}(t) - \tilde{x}^{\tilde{n}(m)}(t)| > \delta \right) \\ & \quad \sup_{t \in I_i} |\bar{x}(t) - \tilde{x}^{\tilde{n}(i)}(t)| \leq \delta, 0 \leq i < m \\ & \leq P \left(\sup_{\tilde{n}(m) \leq k \leq \tilde{n}(m+1)} \|\xi_k - \xi_{\tilde{n}(m)}\|_2 > \frac{\delta}{2C_e} \right) \\ & \quad \sup_{t \in I_i} |\bar{x}(t) - \tilde{x}^{\tilde{n}(i)}(t)| \leq \delta, 0 \leq i < m \\ & \stackrel{(a)}{=} P \left(\sup_{\tilde{n}(m) \leq k \leq \tilde{n}(m+1)} \|\xi_k - \xi_{\tilde{n}(m)}\|_2 > \frac{\delta}{2C_e} \right), \end{aligned} \quad (93)$$

where step (a) is due to the independence of noise, i.e., $\xi_k - \xi_{\tilde{n}(m)}$, $\tilde{n}(m) \leq k \leq \tilde{n}(m+1)$ are independent of \hat{x}_n , $0 \leq n \leq \tilde{n}(m)$.

The lower bound of the probability that the sequence $\{\hat{x}_n : n \geq 0\}$ remains in the invariant set \mathcal{I} is given by

$$\begin{aligned} & P(\hat{x}_n \in \mathcal{I}, \forall n \geq 0) \\ & \stackrel{(a)}{\geq} P \left(\sup_{t \in I_m} |\bar{x}(t) - \tilde{x}^{\tilde{n}(m)}(t)| \leq \delta, \forall m \geq 0 \right) \\ & \stackrel{(b)}{\geq} 1 - \sum_{m \geq 0} P \left(\sup_{t \in I_m} |\bar{x}(t) - \tilde{x}^{\tilde{n}(m)}(t)| > \delta \right) \\ & \quad \sup_{t \in I_i} |\bar{x}(t) - \tilde{x}^{\tilde{n}(i)}(t)| \leq \delta, 0 \leq i < m \\ & \stackrel{(c)}{\geq} 1 - \sum_{m \geq 0} P \left(\sup_{\tilde{n}(m) \leq k \leq \tilde{n}(m+1)} \|\xi_k - \xi_{\tilde{n}(m)}\|_2 > \frac{\delta}{2C_e} \right), \end{aligned} \quad (94)$$

where step (a) is due to Lemma 4, step (b) is due to Lemma 4.2 in [21], and step (c) is due to (93). Let $\|\cdot\|_\infty$ denote the max-norm, i.e., $\|\mathbf{u}\|_\infty = \max_l |\mathbf{u}_l|$. Note that for $\mathbf{u} \in \mathbb{R}^D$,

$\|\mathbf{u}\|_2 \leq \sqrt{D} \|\mathbf{u}\|_\infty$. Hence we have

$$\begin{aligned} & P \left(\sup_{\tilde{n}(m) \leq k \leq \tilde{n}(m+1)} \|\xi_k - \xi_{\tilde{n}(m)}\|_2 > \frac{\delta}{2C_e} \right) \\ & \leq P \left(\sup_{\tilde{n}(m) \leq k \leq \tilde{n}(m+1)} \|\xi_k - \xi_{\tilde{n}(m)}\|_\infty > \frac{\delta}{2\sqrt{3}C_e} \right) \\ & = P \left(\sup_{\tilde{n}(m) \leq k \leq \tilde{n}(m+1)} \max_{1 \leq l \leq 3} |[\xi_k]_l - [\xi_{\tilde{n}(m)}]_l| > \frac{\delta}{2\sqrt{3}C_e} \right) \\ & = P \left(\max_{1 \leq l \leq 3} \sup_{\tilde{n}(m) \leq k \leq \tilde{n}(m+1)} |[\xi_k]_l - [\xi_{\tilde{n}(m)}]_l| > \frac{\delta}{2\sqrt{3}C_e} \right) \\ & \leq \sum_{l=1}^3 P \left(\sup_{\tilde{n}(m) \leq k \leq \tilde{n}(m+1)} |[\xi_k]_l - [\xi_{\tilde{n}(m)}]_l| > \frac{\delta}{2\sqrt{3}C_e} \right). \end{aligned} \quad (95)$$

With the increasing σ -fields $\{\mathcal{G}_n : n \geq 0\}$ defined in Appendix D, we have for $n \geq 0$,

- 1) $\xi_n = \sum_{m=1}^n a_m \hat{\mathbf{z}}_m \sim \mathcal{N}(0, \sum_{m=1}^n a_m^2 \mathbf{I}(\hat{\psi}_{m-1}, \mathbf{W}_m)^{-1})$,
- 2) ξ_n is \mathcal{G}_n -measurable, i.e., $\mathbb{E}[\xi_n | \mathcal{G}_n] = \xi_n$,
- 3) $\mathbb{E}[\|\xi_n\|_2^2] = \sum_{m=1}^n a_m^2 \text{tr}(\mathbf{I}(\hat{\psi}_{m-1}, \mathbf{W}_m)^{-1}) < \infty$,
- 4) $\mathbb{E}[\xi_n | \mathcal{G}_m] = \xi_m$ for all $0 \leq m < n$.

Therefore, $[\xi_n]_l, l = 1, 2, 3$ is a Gaussian martingale with respect to \mathcal{G}_n , and satisfies

$$\begin{aligned} \text{Var} [[\xi_{n+m}]_l - [\xi_n]_l] & = \sum_{i=n+1}^{n+m} a_i^2 [\mathbf{I}(\hat{\psi}_{i-1}, \mathbf{W}_i)^{-1}]_{l,l} \\ & \leq \sum_{i=n+1}^{n+m} a_i^2 \frac{C_I \sigma_0^2}{|s|^2} \\ & = \frac{C_I \sigma_0^2}{|s|^2} [b(n) - b(n+m)], \end{aligned} \quad (96)$$

where $C_I \triangleq \max_l \max_{i \geq 1} \frac{|s|^2}{\sigma_0^2} [\mathbf{I}(\hat{\psi}_{i-1}, \mathbf{W}_i)^{-1}]_{l,l}$. Let $\eta = \frac{\delta}{2\sqrt{3}C_e}$, $M_i = [\xi_{\tilde{n}(m)+i}]_l - [\xi_{\tilde{n}(m)}]_l, l = 1, 2, 3$ and $k = \tilde{n}(m+1) - \tilde{n}(m)$ in Lemma 7, then from (95) and (96), we can obtain

$$\begin{aligned} & P \left(\sup_{\tilde{n}(m) \leq k \leq \tilde{n}(m+1)} |[\xi_k]_l - [\xi_{\tilde{n}(m)}]_l| > \frac{\delta}{2\sqrt{3}C_e} \right) \\ & \leq 2 \exp \left\{ -\frac{\delta^2}{24C_e^2 \text{Var} [[\xi_{\tilde{n}(m)+i}]_l - [\xi_{\tilde{n}(m)}]_l]} \right\} \\ & \leq 2 \exp \left\{ -\frac{\delta^2 |s|^2}{24C_I C_e^2 [b(\tilde{n}(m)) - b(\tilde{n}(m+1))] \sigma_0^2} \right\}. \end{aligned} \quad (97)$$

Combining (94), (95) and (97), we have

$$\begin{aligned} & P(\hat{x}_n \in \mathcal{I}, \forall n \geq 0) \\ & \geq 1 - 6 \sum_{m \geq 0} \exp \left\{ -\frac{\delta^2 |s|^2}{24C_I C_e^2 [b(\tilde{n}(m)) - b(\tilde{n}(m+1))] \sigma_0^2} \right\}. \end{aligned} \quad (98)$$

To use Lemma 8, we assume that the step-size a_n satisfies

$$b(0) = \sum_{i>0} a_i^2 \leq \frac{\delta^2 |s|^2}{24C_I C_e^2 \sigma_0^2}. \quad (99)$$

Then, from Lemma 8, we can obtain

$$\begin{aligned} & \frac{\exp \left\{ -\frac{\delta^2 |s|^2}{24C_1 C_e^2 [b(\tilde{n}(m)) - b(\tilde{n}(m+1))] \sigma_0^2} \right\}}{b(\tilde{n}(m)) - b(\tilde{n}(m+1))} \\ & \leq \frac{\exp \left\{ -\frac{\delta^2 |s|^2}{24C_1 C_e^2 b(0) \sigma_0^2} \right\}}{b(0)}, \end{aligned}$$

for $b(\tilde{n}(m)) - b(\tilde{n}(m+1)) < b(\tilde{n}(m)) \leq b(0)$. Hence, we have

$$\begin{aligned} & \sum_{m \geq 0} \exp \left\{ -\frac{\delta^2 |s|^2}{24C_1 C_e^2 [b(\tilde{n}(m)) - b(\tilde{n}(m+1))] \sigma_0^2} \right\} \\ & \leq \sum_{m \geq 0} [b(\tilde{n}(m)) - b(\tilde{n}(m+1))] \cdot \frac{\exp \left\{ -\frac{\delta^2 |s|^2}{24C_1 C_e^2 b(0) \sigma_0^2} \right\}}{b(0)} \\ & = b(0) \cdot \frac{\exp \left\{ -\frac{\delta^2 |s|^2}{24C_1 C_e^2 b(0) \sigma_0^2} \right\}}{b(0)} = \exp \left\{ -\frac{\delta^2 |s|^2}{24C_1 C_e^2 b(0) \sigma_0^2} \right\}. \end{aligned} \quad (100)$$

As $C_e = e^{L(T+a_1)}$, $b(0) = \sum_{i>0} a_i^2$, and a_n, T, L are given by (22), (59), (86) separately, we can obtain

$$\begin{aligned} \frac{\delta^2 |s|^2}{24C_1 C_e^2 b(0) \sigma_0^2} &= \frac{\delta^2 |s|^2}{24C_1 e^{2L(T+\frac{\alpha}{N_0+1})} \sigma_0^2 \sum_{i \geq 1} \frac{\alpha^2}{(i+N_0)^2}} \\ &= \frac{\delta^2}{\sum_{i \geq 1} \frac{24C_1 e^{2L(T+\frac{\alpha}{N_0+1})}}{(i+N_0)^2}} \cdot \frac{|s|^2}{\alpha^2 \sigma_0^2}. \end{aligned} \quad (101)$$

In (101), $0 < \delta < \inf_{v \in \partial \mathcal{B}} |v - \hat{x}_b|$, (92) and (99) should be satisfied, where a sufficiently large $N_0 \geq 0$ can make both (92) and (99) true.

To ensures that $\hat{x}_0 + a_1 \left[\mathbf{f} \left(\hat{\psi}_0, \psi \right) \right]_3$ does not exceed the mainlobe $\mathcal{B}(x)$, i.e., the first step-size a_1 satisfies

$$\left| \hat{x}_0 + a_1 \left[\mathbf{f} \left(\hat{\psi}_0, \psi \right) \right]_3 - x \right| < \frac{\lambda}{Md},$$

we can obtain the maximum α as follows

$$\alpha_{\max} = \frac{(N_0 + 1) \left(\frac{\lambda}{Md} - |x - \hat{x}_0| \right)}{\left| \left[\mathbf{f} \left(\hat{\psi}_0, \psi \right) \right]_3 \right|}.$$

Hence, from (101), we have

$$\frac{\delta^2 |s|^2}{24C_1 C_e^2 b(0) \sigma_0^2} \cdot \frac{\alpha^2 \sigma_0^2}{|s|^2} \geq \frac{\delta^2}{\sum_{i \geq 1} \frac{24C_1 e^{2L(T+\frac{\alpha_{\max}}{N_0+1})}}{(i+N_0)^2}} \triangleq C. \quad (102)$$

Combining (98), (100) and (102), yields

$$P(\hat{x}_n \in \mathcal{I}, \forall n \geq 0) \geq 1 - 6e^{-\frac{C|s|^2}{\alpha^2 \sigma_0^2}},$$

which completes the proof.

APPENDIX I PROOF OF LEMMA 6

Apply the discrete Gronwall inequality [24], leading (80) to

$$\left\| \bar{\psi}(t_{n+m}) - \tilde{\psi}^n(t_{n+m}) \right\|_2 \leq C e^{L \sum_{i=1}^m a_{n+i}}. \quad (103)$$

Since $1 \leq m \leq n_T$ and $n_T = \inf \{i \in \mathbb{Z} : t_{n+i} \geq t_n + T\}$, we get

$$\sum_{i=1}^m a_{n+i} = t_{n+m} - t_n \leq T + a_{n+n_T} \leq T + a_1. \quad (104)$$

By combining (103) and (104), we have

$$\left\| \bar{\psi}(t_{n+m}) - \tilde{\psi}^n(t_{n+m}) \right\|_2 \leq C e^{L(T+a_1)}. \quad (105)$$

For $\forall t \in [t_{n+m-1}, t_{n+m}]$, $1 \leq m \leq n_T$, from (54), we have

$$\begin{aligned} \bar{\psi}(t) &= \bar{\psi}(t_{n+m-1}) + \frac{(t - t_{n+m-1}) [\bar{\psi}(t_{n+m}) - \bar{\psi}(t_{n+m-1})]}{a_{n+m}} \\ &= \gamma \bar{\psi}(t_{n+m-1}) + (1 - \gamma) \bar{\psi}(t_{n+m}), \end{aligned}$$

where $\gamma = \frac{t_{n+m} - t}{a_{n+m}} \in [0, 1]$. Then, we can get (106), where step (a) is according to the definition of $\tilde{\psi}^n(t)$ in (56), step (b) is due to (105), step (c) is obtained from (87), and step (d) is obtained by using $\gamma = \frac{t_{n+m} - t}{a_{n+m}}$. Therefore, from (106), we can obtain

$$\sup_{t \in [t_n, t_{n+n_T}]} \left\| \bar{\psi}(t) - \tilde{\psi}^n(t) \right\|_2 \leq \frac{C_{\mathbf{f}} a_{n+1}}{2} + C e^{L(T+a_1)},$$

which completes the proof.

$$\begin{aligned}
& \left\| \bar{\psi}(t) - \tilde{\psi}^n(t) \right\|_2 \\
&= \left\| \gamma \left(\bar{\psi}(t_{n+m-1}) - \tilde{\psi}^n(t) \right) + (1-\gamma) \left(\bar{\psi}(t_{n+m}) - \tilde{\psi}^n(t) \right) \right\|_2 \\
&\stackrel{(a)}{=} \left\| \gamma \left[\bar{\psi}(t_{n+m-1}) - \tilde{\psi}^n(t_{n+m-1}) - \int_{t_{n+m-1}}^t \mathbf{f}(\tilde{\psi}^n(s), \psi) ds \right] + (1-\gamma) \left[\bar{\psi}(t_{n+m}) - \tilde{\psi}^n(t_{n+m}) - \int_{t_{n+m}}^t \mathbf{f}(\tilde{\psi}^n(s), \psi) ds \right] \right\|_2 \\
&\leq \gamma \left\| \int_{t_{n+m-1}}^t \mathbf{f}(\tilde{\psi}^n(s), \psi) ds \right\|_2 + (1-\gamma) \left\| \int_{t_{n+m}}^t \mathbf{f}(\tilde{\psi}^n(s), \psi) ds \right\|_2 + \gamma \left\| \bar{\psi}(t_{n+m-1}) - \tilde{\psi}^n(t_{n+m-1}) \right\|_2 \\
&\quad + (1-\gamma) \left\| \bar{\psi}(t_{n+m}) - \tilde{\psi}^n(t_{n+m}) \right\|_2 \\
&\stackrel{(b)}{\leq} \gamma \int_{t_{n+m-1}}^t \left\| \mathbf{f}(\tilde{\psi}^n(s), \psi) \right\|_2 ds + (1-\gamma) \int_t^{t_{n+m}} \left\| \mathbf{f}(\tilde{\psi}^n(s), \psi) \right\|_2 ds + Ce^{L(T+a_1)} \\
&\stackrel{(c)}{\leq} C_{\mathbf{f}}\gamma(t - t_{n+m-1}) + C_{\mathbf{f}}(1-\gamma)(t_{n+m} - t) + Ce^{L(T+a_1)} \\
&\stackrel{(d)}{\leq} 2C_{\mathbf{f}}a_{n+m}\gamma(1-\gamma) + Ce^{L(T+a_1)} \leq \frac{C_{\mathbf{f}}a_{n+m}}{2} + Ce^{L(T+a_1)} \\
&\leq \sup_{1 \leq m \leq n_T} \frac{C_{\mathbf{f}}a_{n+m}}{2} + Ce^{L(T+a_1)} = \frac{C_{\mathbf{f}}a_{n+1}}{2} + Ce^{L(T+a_1)}.
\end{aligned}$$
